Geomorphology 270 (2016) 184–202

Contents lists available at ScienceDirect

Geomorphology

journal homepage: www.elsevier.com/locate/geomorph

Riverside morphological response to pulsed sediment diversions

Ehab A. Meselhe [a,*], Kazi M. Sadid [a], Mead A. Allison [a,b]

[a] The Water Institute of the Gulf, Baton Rouge, LA 70825, United States
[b] Department of Earth and Environmental Sciences, Tulane University, New Orleans, LA 70118, United States

ARTICLE INFO

Article history:
Received 24 January 2016
Received in revised form 12 July 2016
Accepted 13 July 2016
Available online 16 July 2016

Keywords:
Sediment diversion
Morphology
Sediment budget
Stream power

ABSTRACT

Sediment diversions deliver sediment and fresh water from rivers to surrounding wetland areas as a strategy to build and sustain coastal wetland areas. Numerical modeling of the lower Mississippi River, USA, coupled with detailed field observations are used to provide quantitative information about the morphodynamic behavior of river channels in response to diverting large quantities of water and sediment. This study suggests that reduction in river stream power caused by the extraction of significant amounts of water discharge results in river channel aggradation in the vicinity and downstream of diversions. The aggradation quantities depend on the diversion sand capture efficiency and the diverted water discharge relative to the main river discharge. Additional factors observed to influence the sand capture efficiency include the invert elevation of the diversion intake, placement of the diversion intake on top of a lateral or point bars, and the local degree of the river channel curvature. Notably, the capture efficiency of fine material (silt and clay), to a large degree, is not site specific and is rather influenced by the timing of the diversion structure operations relative to the incoming fine-material hydrograph.

1. Introduction

Key factors influencing riverine morphology within the engineering temporal scale (i.e., years to decades) include sediment supply, sediment grain-size distribution, terrain slope, and channel geometry (Garcia, 2008). Channels continuously adjust their geometry and slope in an attempt to minimize energy expenditure and to achieve an equilibrium state (Garcia, 2008). This equilibrium state would inevitably be impacted by extracting water and sediment from the channels through diversions. Extracting and diverting water from rivers is widely practiced for different purposes, including irrigation, domestic and industrial use, navigation, and hydropower. The analysis presented here focuses on the utility of sediment diversion as a strategy for coastal restoration.

Anthropogenic changes to riverine and deltaic systems (e.g., levees) and natural climate changes (e.g., sea level rise and subsidence) had detrimental impacts on these valuable deltaic and coastal ecosystems. Limiting the supply of water and sediment to these systems can have ominous effects, such as rapid coastal land loss and ecological degradation (Syvitski et al., 2009; CPRA, 2012). One viable strategy for coastal restoration is to reconnect rivers to their receiving basins through diversions of sediment-laden water (Allison and Meselhe, 2010; Gaweesh and Meselhe, 2016). Diversions could provide freshwater, mineral sediment, and nutrients to the receiving basins to sustain and build new wetland areas. However, careful consideration should be given to understanding the morphodynamic response of rivers to the extraction of water and sediment. For example, the water diversion from the Ganges River for navigation in the Hoogly River in India has significantly reduced the downstream flow in the Ganges-Brahmaputra reach in Bangladesh, resulted in shoaling in distributary channels, and increased salinity intrusion into the deltaic basin (Mirza, 1998; Rahman and Varis, 2009; Kamruzzaman et al., 2012). The Teesta River, another transboundary river between Bangladesh and India in the Brahmaputra basin, has diversions in India and in Bangladesh for irrigation purposes. The downstream diversion in the Teesta River often receives an inadequate amount of water for irrigation because of upstream water diversions (Rahman and Varis, 2009). In the Yellow River in China, the upstream withdrawals of water result in a significantly reduced flow to the delta during the dry season (Fan et al., 2006).

The focus of this study is to explore and investigate the impact of diversions on the sediment transport capacity and morphology of channels. Further, the study investigates how to implement and operate diversions in a manner that would minimize the impact on morphology, or at least adequately quantify these impacts. In navigable channels, ensuring that these morphological changes do not significantly interfere with navigation activities is important. Specifically, factors that impact the sand capture efficiency and govern the river response to large diversion pulses are investigated here. Additional factors investigated here include placement of the diversion intake relative to lateral sand bars, the potential loss of stream power, and the strength of the local secondary motion. Further, the utility of numerical models to estimate sediment budgets and to quantify the overall response of rivers to pulsed diversions are demonstrated. The lower Mississippi River was selected

* Corresponding author.
E-mail address: emeselhe@thewaterinstitute.org (E.A. Meselhe).

http://dx.doi.org/10.1016/j.geomorph.2016.07.023
0169-555X/

for this study because of the availability of a suitable field observation data set. However, the analysis and findings are relevant to many riverine and deltaic systems.

2. Background

The Mississippi River delta has an area of ~25,000 km^2 and consists of wetlands, bayous, shallow bays, and emergent ridges within the system (Coleman et al., 1998). The coastal shorelines of Louisiana originated in the deltaic system of the Mississippi River in the late Holocene period (6000 yBP to present; Coleman et al., 1998). The Mississippi delta region has been experiencing one of the highest land loss rates (Gagliano et al., 1981; Day et al., 2000). The maximum land loss rate was 102 km^2/y in 1970, then it decreased between the years 1990 to 2000 to a loss of 61 km^2 (Barras et al., 2003). After 2000, two hurricanes (Katrina and Rita) caused a combined 565 km^2 (218 mile^2) of land loss and highlighted the impact of cyclonic storms in coastal land loss (Barras, 2009). The U.S. Geologic Survey (USGS) also investigated the historical wetland loss after Katrina and Rita (29 August and 24 September 2005, respectively). Based on land-water conditions in 1956, USGS estimated land loss of 3540 km^2 (1367 mile^2) over 49 years duration (1956–2005; Barras, 2006). Previous studies have determined that the causes of wetland loss in south Louisiana is a combination of anthropogenic (e.g., levee construction, artificial channel cutting, and subsequent expansion, pond creation, urbanization, construction of dams in the upper Mississippi River, oil and gas withdrawal, etc.) and natural mechanisms, including sea level rise, subsidence, salt water intrusion, and wave- and storm- surge related erosion (Britsch and Kemp, 1990; Penland et al., 1992; Turner, 1997; Day et al., 2000, 2007; Reed, 2002; Morton et al., 2003, 2006; Barras, 2006).

The 2012 Louisiana Coastal Master Plan thoroughly investigated the impacts and potential benefits of sediment diversions for restoration purposes. The Master Plan included modeling components of ecohydrology, wetland morphology, and vegetation models (Couvillion and Beck, 2013; Meselhe et al., 2013; Visser et al., 2013). This comprehensive modeling approach provided an assessment of the impact of sediment diversion on wetland geomorphology and ecosystem services (Steyer et al., 2012; Couvillion and Beck, 2013; Rivera-Monroy et al., 2013).

Numerical models supported by extensive field observations have been used to plan and analyze sediment diversions from the Mississippi River into Barataria Bay, Louisiana (Meselhe et al., 2012; Allison et al., 2013, 2014; Ramirez and Allison, 2013). This analysis supplements these previous studies by utilizing a validated numerical model to shed some light on the morphologic response of rivers to diversions. The model will also be used to further the understanding of the dominant and critical parameters that govern sand capture efficiency and response of the river channel to the extraction of water and sediment.

The diversions considered in this study are >1420 cubic meters per second (m^3/s) of water exiting from the main river (Allison and Meselhe, 2010). The term *pulse* refers to the strategy of diverting sediment and water primarily during flood events and reducing or stopping the diversion during average and low flow periods. The definition of a flood event varies from one system to another. In the lower Mississippi River, it is defined as an event with flow discharge >16,990 m^3/s (Meselhe et al., 2012). This threshold has been determined based on numerous field observations identifying this discharge as the impetus for entraining coarse material into suspension (Allison et al., 2013).

3. Modeling approach

A three-dimensional numerical model of the Mississippi River channel supported by detailed field observations is used to perform a thorough analysis of large-scale pulsed sediment diversions. The intent of this analysis is to provide insights into the morphodynamics of the river channel in response to sediment diversions. The process-based Delft3D model is used for this study.

Delft3D is a three-dimensional modeling system that consists of a number of integrated modules to simulate fluid flow, wave generation and propagation, sediment transport, and morphological changes (Lesser et al., 2004; Deltares, 2011). This model has been applied to a wide range of riverine, estuarine, and coastal systems (Sutherland et al., 2003; Edmonds and Slingerland, 2007, 2010; Bos, 2011; Caldwell and Edmonds, 2014). The hydrodynamic and morphodynamic modules of Delft3D are fully coupled computationally where the evolving bathymetry (caused by deposition and erosion) interacts with and influences the flow field and vice versa. This modeling tool allows for long-term simulations of morphological evolution (i.e. years to decades) through the use of numerical acceleration techniques (Lesser et al., 2004; Deltares, 2011).

In this study, the standard k-ϵ turbulence closure model is used. The k-ϵ model is widely used for its relative computational efficiency and adequate performance for a wide range of practical applications (Edmonds and Slingerland, 2007; Meselhe et al., 2012).

The sediment processes of Delft3D-Flow include computing bedload and suspended load transport of coarse and fine sediment (Lesser et al., 2004; Deltares, 2011). The Van Rijn (1984a, 1984b) formulation was used for coarse sediment (Van Rijn, 1984a, 1984b). Previous studies on the lower Mississippi River and basins show that the Van Rijn (1984a, 1984b) formulation is appropriate to calculate the coarse sediment loads with its two main components: suspended loads and bedloads (Edmonds and Slingerland, 2007). We should also note that the Van Rijn (1984a, 1984b) formula is commonly used for noncohesive sediment transport in riverine applications where sedimentation processes induced by waves are not prevalent. For the bedload transport, it solves the equations of motions for individual particles and computes the saltation characteristics as a function of the flow conditions (Van Rijn, 1984a). The computation of the suspended load is based on the depth-integration of the local concentration, local flow velocity, and on the near-bed concentration (known as reference concentration). The Partheniades-Krone formulations (Partheniades, 1965) were used for fine sediment. The method is fundamentally based on calculating critical stresses for erosion and deposition. These stresses essentially drive the erosion and deposition processes of fine sediment. The interested reader can find full description of these methods and related formulation in Partheniades (1965) and Van Rijn (1984a, 1984b).

Based on the observations by Allison et al. (2013), three standard sand classes were considered in this study: very fine (62.5–125 μm), fine (125–250 μm), and medium (250–500 μm). Notably, only D_{50} was provided as a model input parameter based on field observations of the grain-size distribution of the suspended sediment material as well as bed grab samples. The numerical model then generates a distribution curve internally.

The fine sediment considered here was classified into two fractions, clay and silt, each with different settling velocities and critical shear stresses.

The model, supported by field observations, will be used to study an existing diversion on the lower Mississippi River to serve as an analogue of how the river morphologically responds to pulsed water and sediment diversion. The model will also be used to predict how the river would respond to a proposed sediment diversion as part of the State of Louisiana Coastal Master Plan (Fig. 1).

4. Analogue

A lower Mississippi River reach with an approximate length of 29 km (river kilometer [RK] 191.50 through RK 220.50 measured from the river mouth known as the Head of Passes) immediately upstream of New Orleans, LA, is used as an analogue to investigate the riverside morphological response to a pulsed diversion of water and sediment. This location is referred to here as the *BC model* (Fig. 1). The BC model

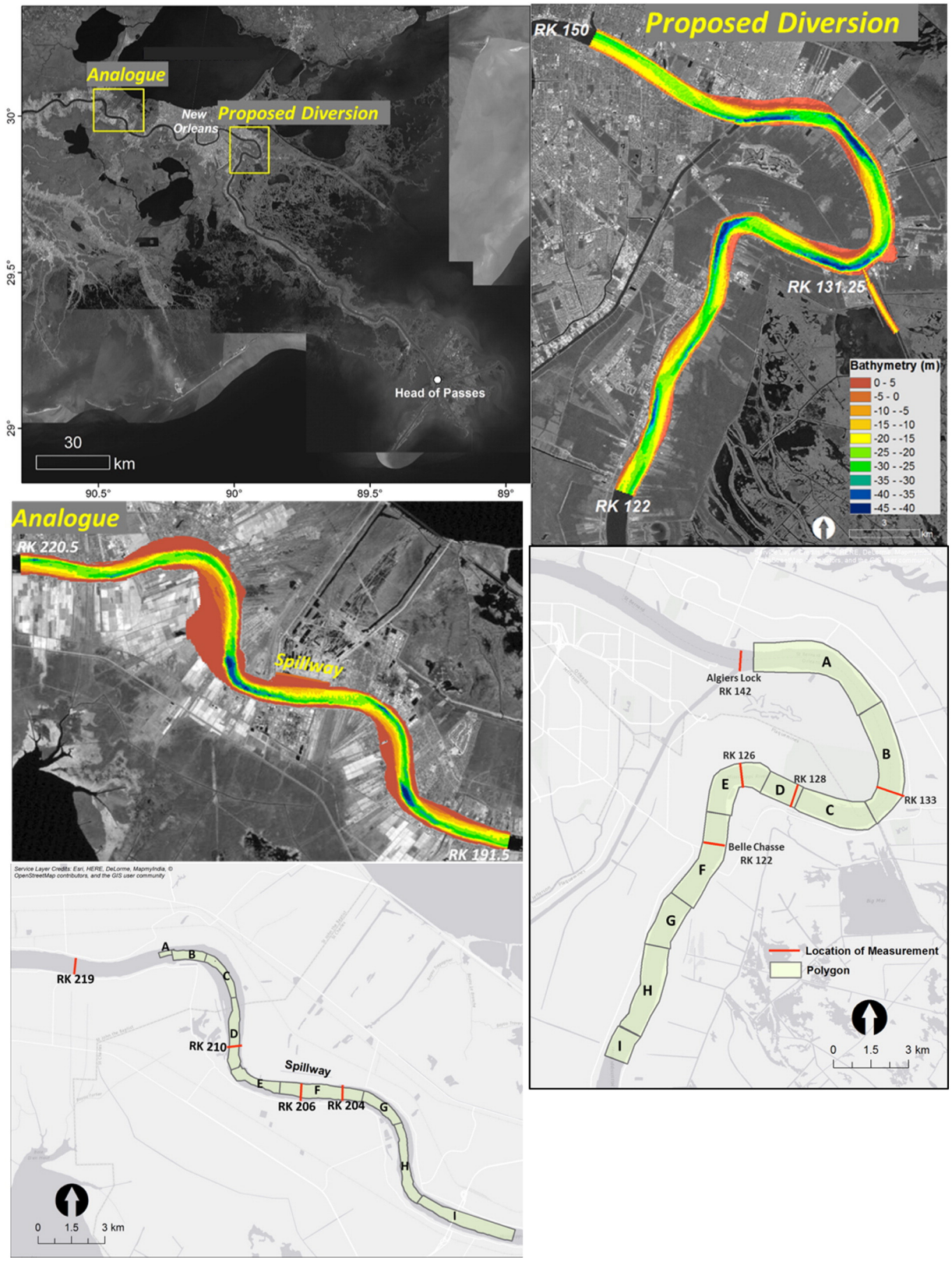

Fig. 1. Study area maps showing the location of the analogue and the proposed sediment diversion, the bathymetry of both locations, the locations used to compare model output to measurements, and the polygons used to analyze the deposition and erosion patterns.

includes the Bonnet Carré (BC) spillway, a flood control structure, and a small portion of Lake Pontchartrain. The Bonnet Carré spillway is an existing gated flood control diversion designed to protect the city of New Orleans from extreme river floods. It diverts Mississippi River floodwater into the Gulf of Mexico through Lake Pontchartrain when the river reaches 35,400 m^3/s discharge at the U.S. Army Corps of Engineers (USACE) Tarbert Landing gage (USACE station ID: 01100Q-RK 491). Since its construction in 1937, the spillway has been operated 11

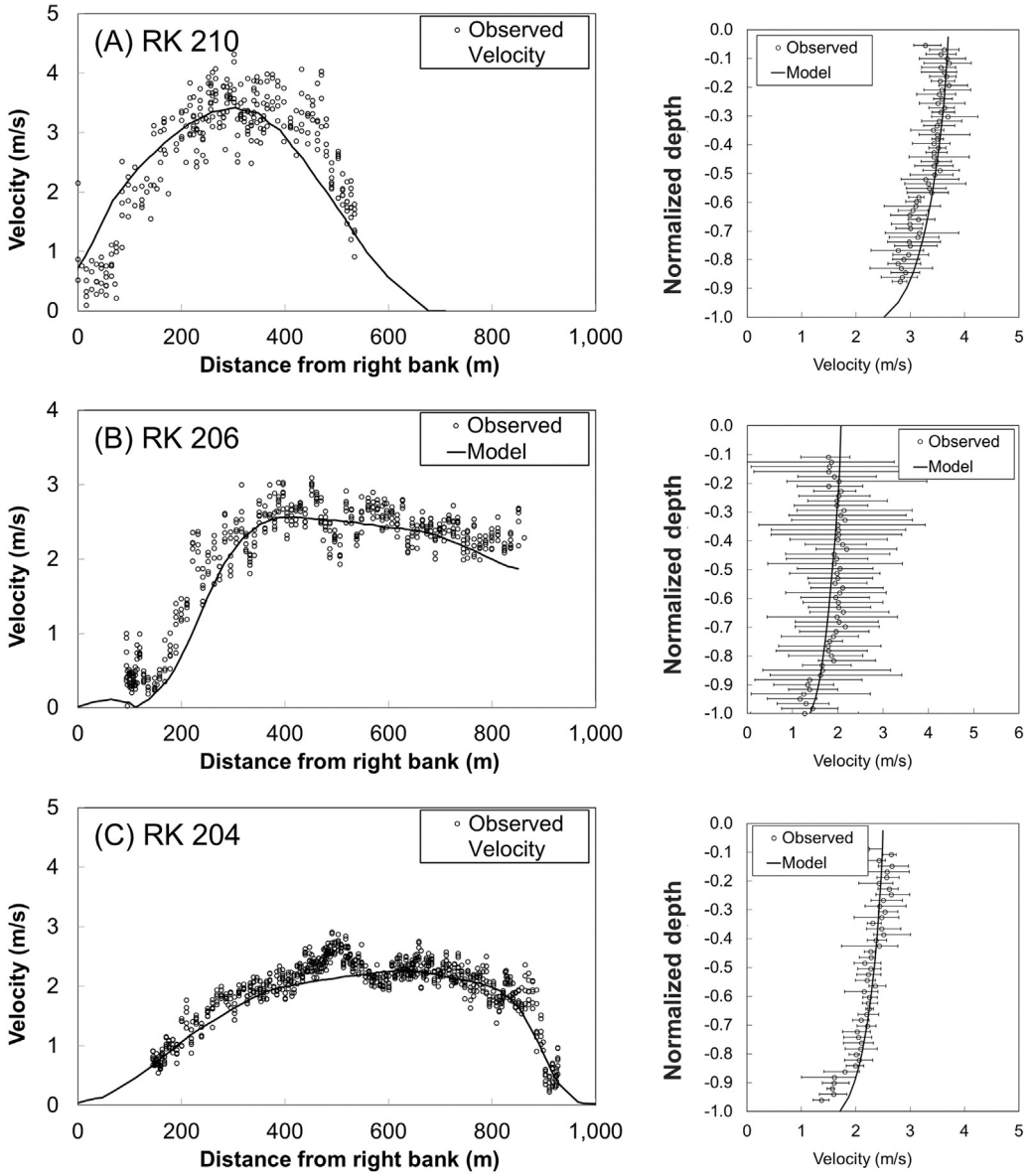

Fig. 2. Comparison between the model - derived velocity and field observations.

times during flood events, most recently in the 2016 Mississippi River flood.

To investigate the river's response to pulsed diversions, three BC opening events (1997, 2008, and 2011) were analyzed. The spillway is ~2000 m wide and has 350 bays. All elevations in this modeling effort are referenced to the North American Vertical Datum 1988 (NAVD88). The bottom elevation for 174 bays is at 4.5 m NAVD88 and the remaining is at 5.1 m NAVD88, whereas the riverbed elevation near the thalweg reaches elevations lower than −50 m NAVD88 (Fig. 1). In essence, the spillway draws water from the upper layers of the water column where sand concentrations are typically low.

4.1. Model setup

The curvilinear grid used for this analysis had a resolution ranging from 30 m × 30 m to 30 m × 90 m. The water flux upstream of the model is estimated using the daily discharges measured by the USGS at Baton Rouge, LA (USGS 0737400; RK 367.5). The water volume calculations within the river reach under consideration used the water stage data of the U.S. Army Corps of Engineers (USACE) from Bonnet Carré (station ID: 01280 – RK 204), the Carrollton (station ID: 01300 – RK 165), and the water stage data at West End (station ID: 85634) to represent the water level in Lake Pontchartrain (Fig. 1). We should clarify that the model included the floodway downstream of the Bonnet Carré spillway only to set up proper tailwater conditions. The analysis and emphasis remained to be on the riverside sediment and flow dynamics. The suspended sediment concentrations were estimated daily and prescribed as an upstream boundary condition based on rating curves at Baton Rouge (Allison et al., 2012) and are shown below in Eqs. (1) and (2). Notably, rating curves reflect the relationship between the sediment concentration and flow rate but will not capture hysteresis. The only way to capture hysteresis is to impose a sediment load time series, which is not available.

$$\textit{Suspended Sand Load} = a\left[1-e^{(-bQ_w)}\right] + c\left[1-e^{(-dQ_w)}\right] \quad (1)$$

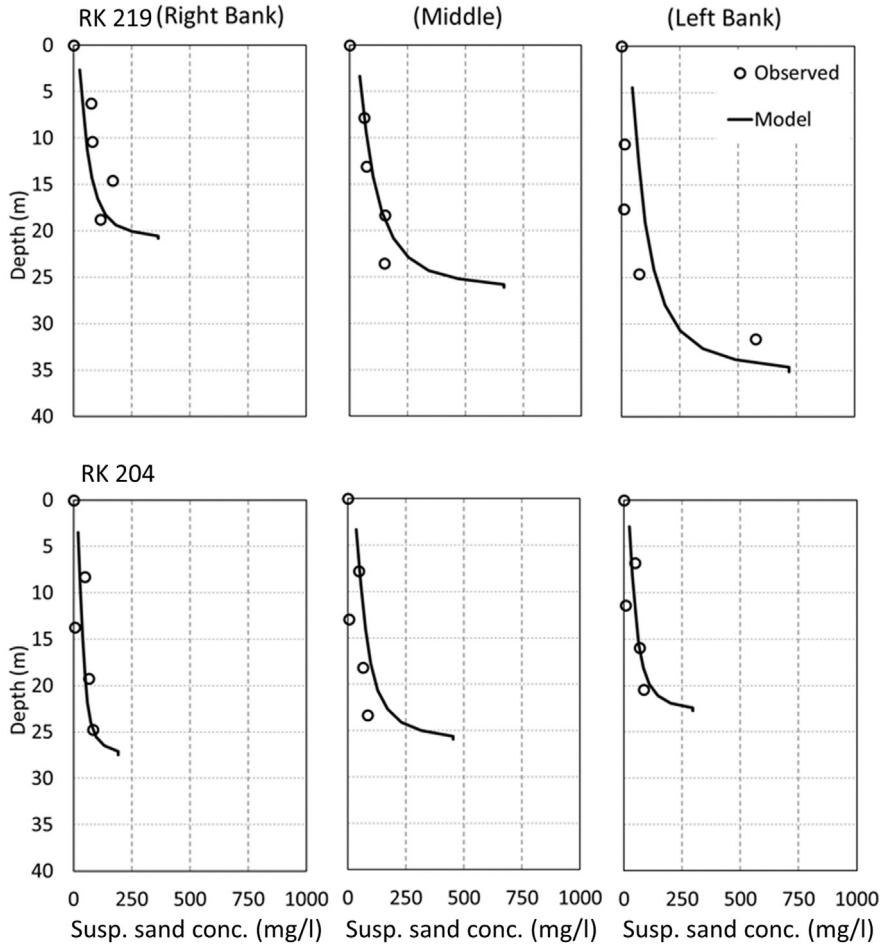

Fig. 3. Comparison between model results and vertical sand profiles measured on 21 May 2011 at RK 219 and 204.

where,

$a = -2.145 \times 10^{5}; b = 2.855 \times 10^{-6}; c = 3.261 \times 10^{9};$
$d = 1.24 \times 10^{-10}$

$$\text{Suspended Fine Load} = AQ_w{}^{B} \quad (2)$$

where,

$A = 1.71; B = 1.17$

A multilayer bed composition model consisting of all the sediment fractions was defined based on the collected bed grab samples. The underlayer substrates were comprised of fine (~10%), medium (~60%), and coarse (~30%) sands. The design of substrates was supported by field observations (Allison et al., 2013). The field observations (Allison et al., 2013) also indicate areas of exposed relict material highly resistant to erosion in the river bottom. An examination of the geometry of these relict areas in the field data allowed for the assumption that bed elevation below −35 m NAVD88 was considered to be bedrock. The remaining areas of the river bottom had variable sediment thickness where it reached the largest value between the thalweg and the bar. The sediment layer thickness gradually decreased from the bar to the banks of the river. This design was prepared based on professional experiences with the lower Mississippi River surveys and using the multibeam surface of the river bottom, which shows relative changes in bedforms between crossing and bend sections (Allison et al., 2014).

4.2. Model calibration and validation

The BC model was calibrated utilizing a field data set associated with a large flood event and the Bonnet Carré spillway opening between 1 May and 25 June 2011. This data set included multibeam bathymetric mapping of the BC reach of the Mississippi River channel, acoustically measured flow fields, suspended and bedload transport rates, and bed sediment character. This data set is presented in detail in Allison et al. (2013). Boat-based field observations were collected on 9–11 May 2011 immediately prior to the opening of the Bonnet Carré spillway, on 20–22 May 2011 with the structure fully open, and again on 23–25 June 2011 immediately after the structure closure. First, the hydrodynamic component of the model was calibrated against observed flow velocity profiles, water level, and discharge. After the hydrodynamics were calibrated, the sediment transport component was compared against observations of sediment loads and concentration profiles. The Manning bed roughness coefficient (n) was used as a calibration parameter for water stage and flow patterns. The large water discharge in the 2011 flood yielded large suspended and bedload flux rates. The high sand flux created large dunes (20–100 m wavelength, 1–4 m height) on the bar areas of the riverbed, resulting in a higher flow resistance. To accommodate these features, a spatially variable roughness map was selected. The map consisted of a relatively smooth main channel ($n = 0.024$) and relatively rough areas on top of sand bars ($n = 0.05$). Also, during the flood events, the water flux from the Baton Rouge station was corrected by a factor of 0.925 to account for rating curve discrepancies and water losses between Baton Rouge and Bonnet Carré (Kolker et al., 2013).

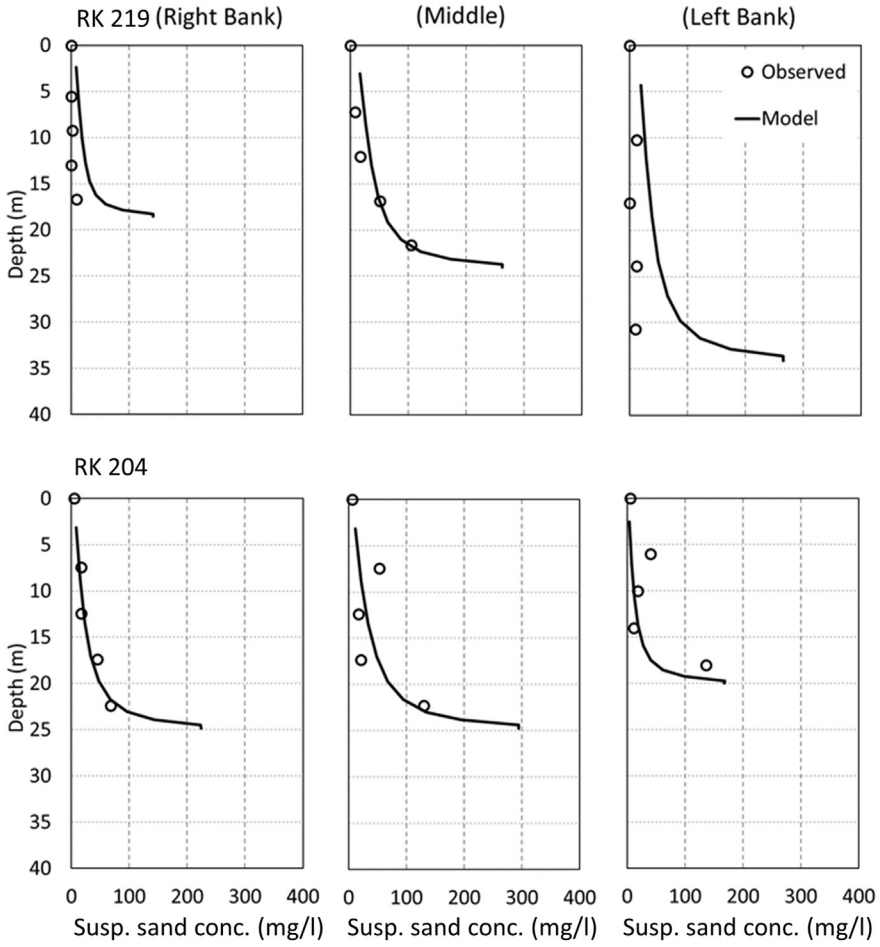

Fig. 4. Comparison between model results and vertical sand profiles measured on 22 June 2011 at RK 219 and 204.

Sediment transport calibration was guided by field measurements available at two locations: one upstream (RK 219) and another downstream (RK 204) of Bonnet Carré spillway. The measurements were taken at two different occasions: one during the peak flood (21 May) and the other the post-flood period (22 June) of 2011. One of the parameters in the Delft3D sediment module, namely the Reference height, was a key calibration parameter for suspended sand concentrations. This parameter varies with the bedform height. According to a previous study by Khaiashy et al. (2010), the bedform height in the study area under consideration should be around 2.25 m. Range of values from 1 to 4 m were tested for the reference height. A uniform reference height of 2 m produced reasonable numerical results compared to the field measurements.

To gain computational efficiency, the spillway gate operations during the flood event were simplified in the model. In practice, the gates are opened gradually over the span of several days. That process was simplified (i.e., all the gates were assumed to be open) and the diverted flow was mainly driven by the head-difference between the river and Lake Pontchartrain. To ensure that this assumption did not undermine the integrity of the analysis, a test with the detailed operation was done initially and confirmed that the impact of simplifying the spillway operation on the analysis was not significant for the purpose of this analysis.

After the calibration for the 2011 flood event, the model was validated for the spillway openings in 1997 and 2008. For the 1997 event, the water and sediment fluxes were measured at the fore bay, the Airline Highway, and at I-10 (see Fig. 1, for location of the stations). However, the measurements were taken only at the Airline Highway in the 2008 flood event.

Fig. 2 shows a comparison between field ADCP and model-driven velocity profiles (locations are shown in Fig. 1). The modeled velocities are in reasonable agreement with the field measurements. Figs. 3 and 4 show a comparison between the modeled and measured vertical sand profiles. The model results are in reasonable agreement with the measurements. Comparison between the measured and calculated sediment fluxes at RK 219 and RK 204 in Fig. 5 also shows a reasonable agreement between the measured and calculated fluxes. Given the challenges of capturing sediment dynamics, a ratio between modeled and measured sediment load in the range of 0.5 and 2 is typically accepted (Meselhe and Rodrigue, 2013). Fig. 5 also shows the decrease in the sediment flux—especially in the suspended load—between the upstream and downstream sections of the diversion. Some of the sediment was extracted through the diversion, and some was deposited between the two locations. A sediment budget discussed later will provide further insights on the fate of sediment in this river reach.

Further, the model predictions of water discharge and sediment loads extracted through the spillway were compared against field measurements for the 2011, 2008, and 1997 flood events (Fig. 6). As shown in Fig. 6, the predicted water volume and the fine sediment load for the three flood events compare favorably against the field measurements (Fig. 6, top and middle panels).

The model predicted the extracted sand load through the spillway for the 1997 flood event well, but overestimated the load for the 2011 and 2008 events. One source of uncertainty of the sand load extracted

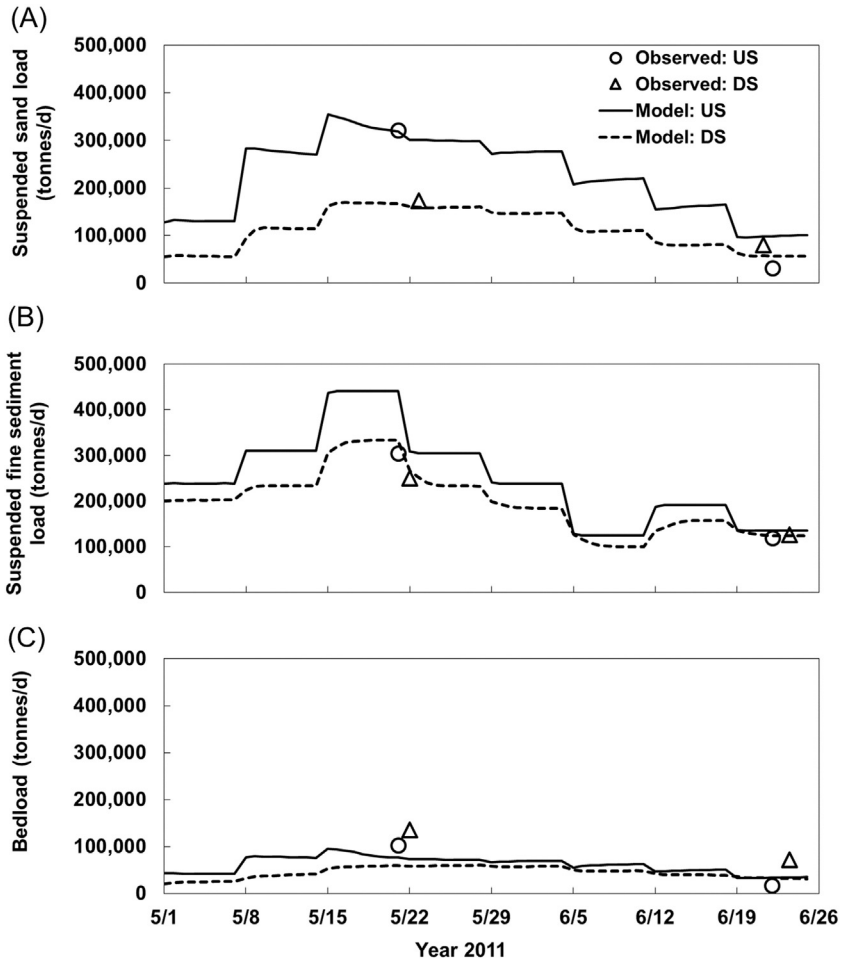

Fig. 5. Comparison of sediment loads between the model results and field observations at US (RK 219) and DS (RK 204) of the Bonnet Carré spillway: (A) suspended sand loads, (B) fine sediment loads, and (C) bedloads.

through the spillway is the amount of sand deposited in the forebay area of the spillway. The surface elevation of this area as specified in the model may not capture all the dredging activities commonly practiced to clear the area from deposits of previous flood events.

To further evaluate the model ability to capture the morphological response of the river to a large pulsed diversion of water and sediment, the deposition and erosion quantities were calculated. The deposition and erosion quantities were measured in the field through repetitive multibeam surveys (Allison et al., 2013). The mutlibeam maps were gathered in May 2011 and June 2011 to bracket the bed changes during the flood event. Additional multibeam mapping of the riverbed was done in June 2012 to investigate the fate of the deposited material after one full year. The comparison between the model predictions and field observations is shown in Fig. 7. The multibeam surveys in polygons A, B, and C were not fully surveyed in the field (Allison et al., 2013), and as such, a direct comparison with the model results was not possible.

Overall, the calculated and measured deposition/erosion patterns are consistent. The uncertainty band around the field observations shown in Fig. 7 corresponds to a random error (representing the measurement uncertainty) of ~±20 cm at any given point in the multibeam map, which is an operational error derived from comparison of remapped swaths, as opposed to the much smaller theoretical limits of the mapping system. The model results as well as the field observations showed that significant accretion occurred in front of the spillway in polygon F, while little to no erosion occurred in polygon E upstream of the spillway. Further, the model estimated ~3×10^6 m^3 was eroded from polygon F and migrated downstream (polygons G and H) during the period of June 2011 to June 2012 (Fig. 7B). This erosion process was likely induced by three moderate flood peaks of 22,650–24,650 m^3/s that occurred during the period of December 2011 to April 2012. Since a continuous sediment record does not exist upstream of the diversion, thus the upstream sediment loads and the size distribution had to be estimated based on a rating curve at Baton Rouge. As such, the model had continuous supply of sediment for consecutive flood events as per the rating curve, whereas in reality sediment supply might be limited for successive flood events, and sediment starved river flows could be relatively more erosive. Despite these uncertainties, the calculations indicated trends consistent with the field observations. Overall, the model captured the most prominent morphological changes that occurred during that flood period as well as during the full year following the flood event, i.e. the wash out and downstream migration of the deposited material.

The 1997 and 2008 flood events of 43 and 37 days, respectively, resulted in deposition volumes in polygon F of similar magnitude to that of the 2011 flood event; i.e., ~4×10^6 m^3 (Fig. 7C). Observational channel studies equivalent to 2011 do not exist for these earlier events.

In addition to the visual evaluation of the model agreement with field observations, a statistical analysis was conducted to evaluate the model performance (Meselhe and Rodrigue, 2013). Three goodness-of-fit statistics: the root mean square error percentage, the Pearson product-moment correlation coefficient, and the bias percentage were

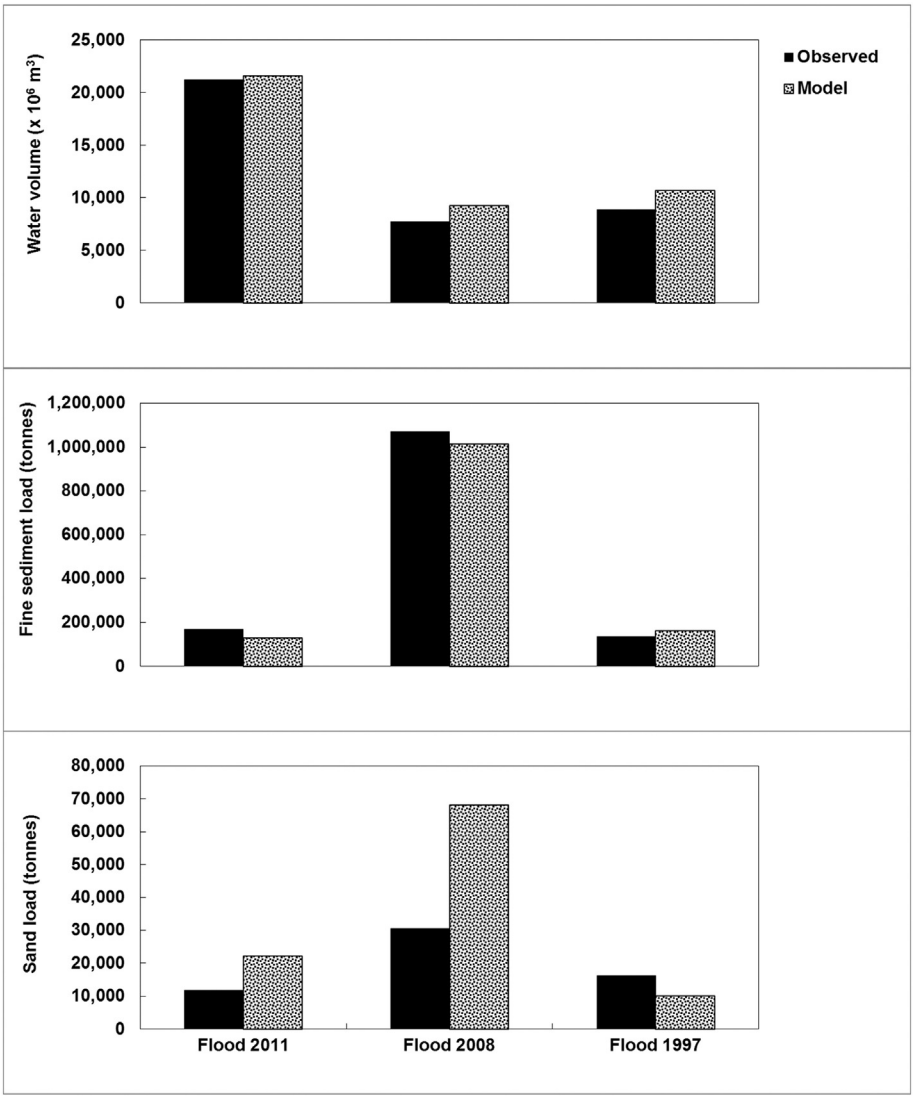

Fig. 6. Comparisons between the model results and field observations for diverted flow and sediment loads for the 2011, 2008, and 1997 floods.

calculated (Table 1). Root mean square error (RMSE) is calculated as the square root of the average of the squared residuals. The residuals are the differences between the predicted and observed data. A small RMSE percentage indicates a better agreement between the predicted and observed data. Calculating the model percent bias is important to verify if the model is consistently over- or underestimating critical quantities. Positive BIAS% refers to model bias toward overestimation and negative BIAS% indicates a bias toward underestimation. The Pearson product-moment correlation coefficient refers to a measure of the phasing between the predicted and observed data. As seen in Table 1, the model performed well against the measurements, but it overestimated the extracted sand load as see in the RMSE%. The uncertainties discussed above related to the upstream boundary conditions as well as the available sand deposit in the forebay area contribute to the high RMSE listed in Table 1.

4.3. Model applications and analysis

Additional insights can be gained through the development of sediment budgets. A separate budget has been developed for sand and fines (silt and clay). The 2011 event budget shows the cumulative sediment mass and bulk volume based on a dry density of 1600 kg/m^3: (i) entering/leaving the river segment studied here, (ii) passing through the diversion structure, and (iii) eroding or depositing within the river channel. The model sand budget showed that 29% of the inflowing sand load, which was about 5.1 million tonnes, was deposited on the riverbed and 44% exited through the downstream section (Table 2; Fig. 8). The model-based sand budget also shows that 17% of the inflowing sand load was deposited on the forebay and 10% passed through the spillway structure. The diverted flows and sediment loads were included in Table 2 to provide a complete budget. However, the emphasis of this effort is on the riverside morphologic response to pulsed diversions.

The model fine sediment budget (clay and silt finer than 62.5 μm) indicates that 4% of the entering fine sediment load was deposited and 87% exited the system. The model also shows that 2 million tonnes of fine materials (12%) were entrained from the forebay area by the flood flow diverting through the spillway. Nearly 3.5 million tonnes (21%) of silt and clay were diverted through the spillway. Fabre (2012) documented that the uppermost 2 cm of the bed in Lake Pontchartrain had average grain sizes within the fine to medium silt range (<64 μm) before, during, and after the operation of the spillway in 2011. Also, the total fine sediment deposition in Lake Pontchartrain

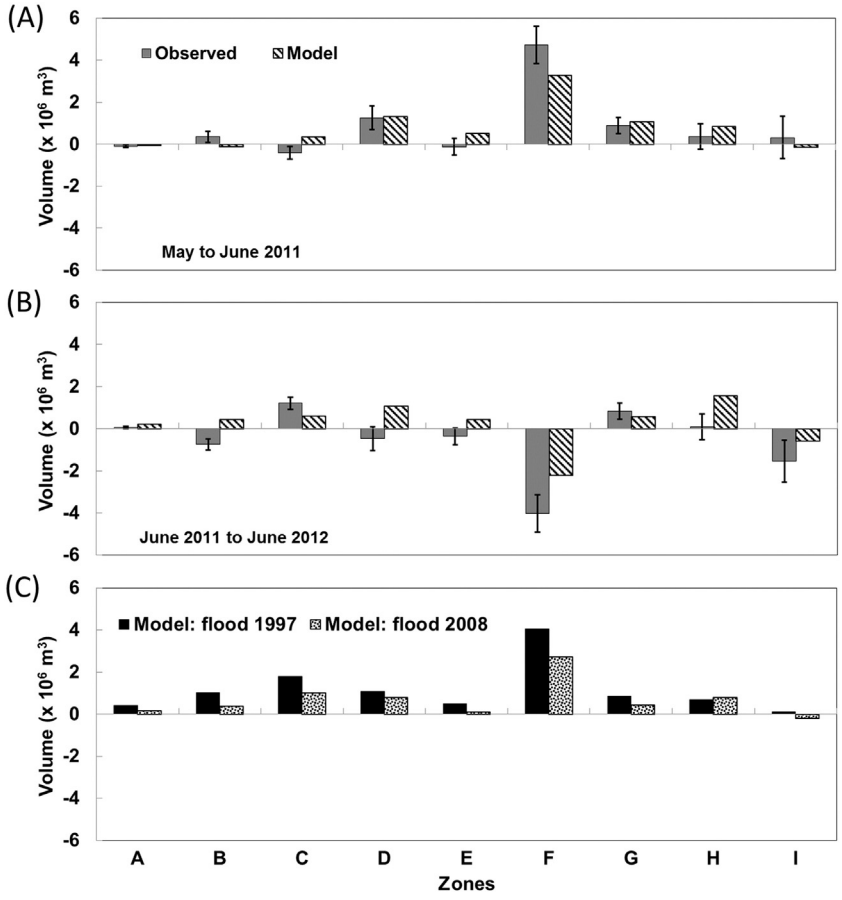

Fig. 7. Erosion and accretion volumes: (A) comparison between measured vs. estimated for the Bonnet Carré opening during the 2011 flood, (B) comparison between measured vs. estimated from June 2011 to June 2012, and (C) estimates for the Bonnet Carré openings during the 1997 and 2008 flood events.

between 8 May and 8 July 2011 was 2.45 ± 1.35 million tonnes, estimated by changes in ^{7}Be inventories. These findings are consistent with and support our model results.

4.4. Discussions

A sediment-water ratio (SWR) was used to quantify the capture efficiency (Meselhe et al., 2012). This ratio can be used as an indicator for the potential riverine deposition resulting from a diversion pulse. This ratio is defined as follows:

$$\mathrm{SWR} = \frac{\text{Sediment Load Diverted/Sediment Load in the River}}{\text{Water Discharged Diverted/Water Discharged in the River}} \quad (3)$$

A higher SWR value indicates a higher sand concentration in the diverted water compared to the average sand concentration of the main river, thereby lowering the potential for undesirable deposition in the river.

The sand concentration is spatially variable within the channel cross section. Typically it is highest near the bed, on top of sand bars, and near the inner bank of a bend compared to the outer bank. Hence, the sand capture efficiency is significantly influenced by the location and depth of sediment diversions. Therefore, locating the intake of proposed diversions on top of sand bars is important. Certainly sand concentration is also variable temporally. It is directly proportional to the water discharge, and if multiple flood events occur in the same year, the local sand sourcing may be exhausted and the same water discharge would correspond to lower sand concentration in later events in the same year compared to earlier events. But in any given flood event, sand concentrations are relatively higher on top of sand bars compared to elsewhere in the cross section.

Fine sediment, on the other hand, is distributed fairly uniformly within a channel cross section. The fine sediment concentration also exhibits significant temporal variation. It is highest on the rising limb of a flood event (Mossa, 1989; Allison and Meselhe, 2010; Allison et al., 2014). Therefore, in order to maximize the amount of fine material captured, sediment diversions should be operated during the rising limb of a flood event. The capture efficiency of fine material is always near unity, and the key factor to maximize the amount of fine material diverted is the relative timing of operating a diversion relative to the incoming fine material hydrograph.

The SWR for the spillway was calculated from the model results for the pulse of the 2011, 2008, and 1997 flood events (Fig. 9). The ratio for sand was ~0.5 during all three events. This low SWR of sand partially explains the significant deposition downstream of the spillway. The low SWR is caused by the high invert elevation of the spillway causing it

Table 1
Model performance statistics for the BC model.

Model Output: May–June 2011	Bias %	RMSE%	Correlation coefficient
Velocity (transverse profile)	−4.6%	18.9%	0.9
Velocity (Vertical Profile)	−19.5	21.5%	0.8
Water level	−1.5%	0.9%	1.0
Discharge extracted through the spillway	3.0%	11.0%	0.9
Sand load extracted through the spillway	22.0%	115.0%	0.9
Fine load extracted through the spillway	13.0%	32.0%	0.8

Table 2
Sediment budget for the BC model for the 2011 flood.

Sediment type	Sediment	Inflow at the US of the spillway	Outflow at the DS	Deposited on the riverbed	Deposited in fore bay	Flow through the spillway
Sand	Total Mass (10^6 tonnes)	17	7	5	3	2
	% with U/S		44%	29%	17%	10%
Fine sediment	Total Mass (10^6 tonnes)	15	13	1	−2	3
	% with U/S		87%	4%	−12%	21%
Total	Total Mass (10^6 tonnes)	33	21	6	1	5
	% with U/S		64%	17%	3%	16%

to draw water from the upper layers of the water column that are not sand rich.

Further insights into the morphological response of the river to this pulse can be gained by analyzing the stream power. Stream power is the rate of energy dissipation along a river per unit length and is defined as $\gamma_w Q_w S$, where γ_w is water weight, Q_w is total water discharge, and S is the energy slope (Bagnold, 1966). To avoid excessive deposition in the river channel, a reduction in the stream power should be accompanied by a proportional reduction in the sediment load. Fig. 10 shows model-predicted water surface profiles: one at a river discharge of 31,000 m^3/s with no flow diversion through the spillway, and a second at a river discharge of 39,500 m^3/s with a peak diversion discharge of ~8928 m^3/s. The figure also shows a clear decline in the water surface slope downstream of the diversion when it is operational. A one-dimensional model was used to estimate the energy surface slope upstream and downstream of the diversion. A reach of ~135 km was used to estimate the slope upstream of the diversion and a 63-km reach was used to estimate the downstream slope. The reason for using long river reaches is to establish a reliable estimate of the slope. A shorter reach may result in a less reliable estimate of the slope.

The reduction of discharge and slope owing to the diversion resulted in a ~47% loss of stream power. This significant reduction in the stream power accompanied by a low removal of sand (SWR < 0.5) resulted in the rapid aggradation downstream of the diversion. Perhaps the question remains if a high sand capture efficiency would offset the loss of stream power and prevent the aggradation in the river channel downstream of a large diversion. The next section of this paper presents a proposed diversion with a high sand capture efficiency and might shed some light on the answer to this question.

5. Proposed sediment diversion

The morphodynamic model used to study the analogue presented in the previous section of this paper is used to provide insight on the morphologic riverside response to a proposed sediment diversion. The proposed diversion is located near the English Turn (RK 125) and is intended to divert Mississippi River sediment into the upper Breton Sound Basin. The term *ETB model* refers to a 27-km reach (RK 150 through RK 122), including the English Turn bend (ETB) near RK 125, immediately downstream of New Orleans, LA (Fig. 1). The diversion is designed with the outfall invert at −12.19 m NAVD88, located on top of a sand bar and at the inside of a bend to draw water from deeper sand rich layers (Meselhe et al., 2012; Allison et al., 2014). The design capacity of the diversion is 7080 m^3/s (250,000 cfs) of water when the river discharge is at 28,316 m^3/s (1×10^6 cfs). Smaller capacities of 3540 m^3/s (125,000 cfs) and 2124 m^3/s (75,000 cfs) with the same invert elevation were also studied.

5.1. Model setup

The grid resolution in the ETB model ranged from 20 m × 40 m to 40 m × 80 m. The upstream boundary of the model is provided using flow at Belle Chasse (USGS station ID: 07374525-RK122) near RK 122. The water volume within the river reach of the ETB model is calculated

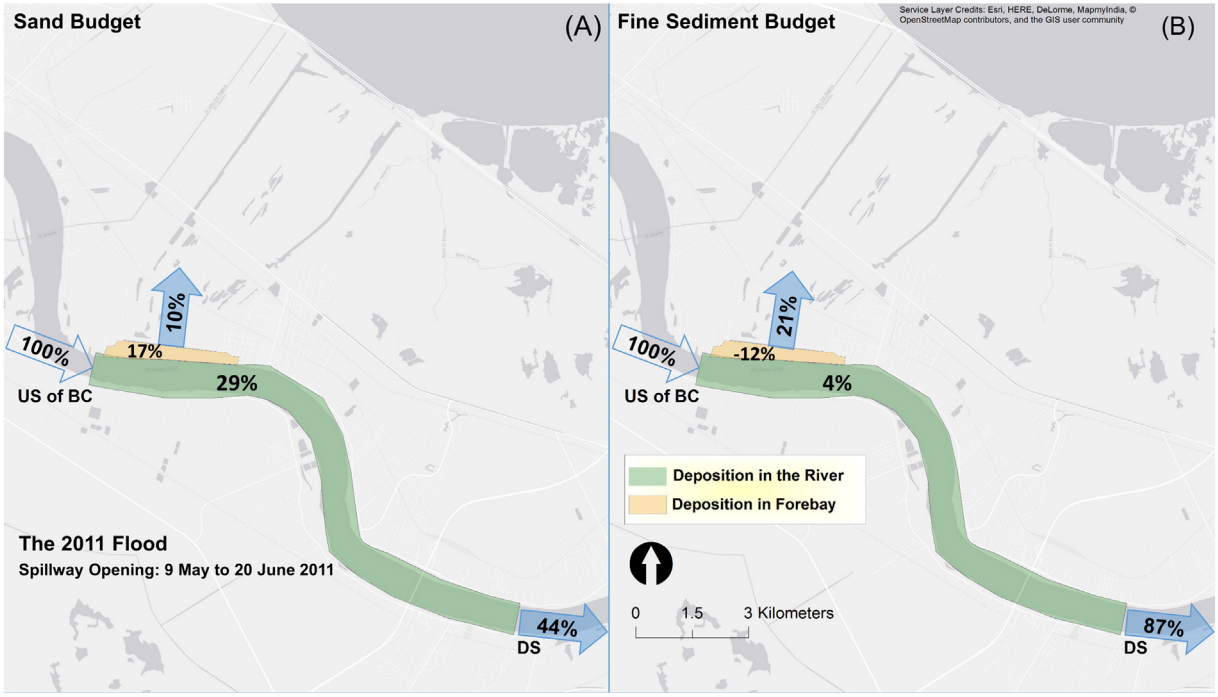

Fig. 8. Model - predicted sediment budgets for the period of May 2011 through June 2011: (A) sand budget and (B) fine sediment budget.

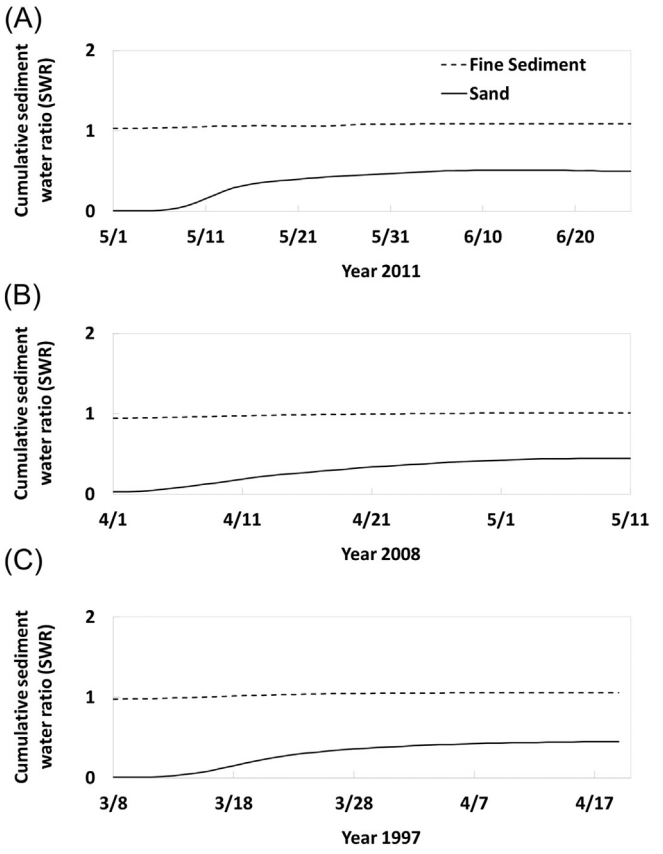

Fig. 9. Cumulative SWR for the analogue (Bonnet Carré spillway) during the flood events as predicted by the numerical model: (A) 2011, (B) 2008, and (C) 1997.

using information at the Belle Chasse gage (USGS station ID: 07374525, RK 122) and Algiers Lock (USACE station ID: 01380-RK 142). The water and sediment passing through the diversion are gravity-driven with stage boundary condition at the end of the outfall channel. The Coastwide Reference Monitoring System (CRMS; Steyer et al., 2003) stations located near the outfall were used to estimate the water level in the receiving basin.

The suspended sediment concentration at Belle Chasse was estimated daily based on a rating curve and prescribed as an upstream boundary. The rating curves for Belle Chasse documented in Allison et al. (2012) were updated using USGS measurements for the period 2008–2012. The equations of the rating curves for coarse and fine sediment are given in Eqs. (4) and (5), respectively.

$$\text{Suspended Sand Load} = a\left[1-e^{(-bQ_w)}\right] + c\left[1-e^{(-dQ_w)}\right] \quad (4)$$

where, $a = 7.716\times10^{7}$; $b = 2.485\times10^{-7}$; $c = -5.748\times10^{5}$; $d = 4.122\times10^{-5}$

$$\text{Suspended Fine Load} = AQ_w{}^{B} \quad (5)$$

where, $A = 0.002$; $B = 1.86$.

Q_w is river discharge in m^3/s, and sediment load is in metric tonnes/d.

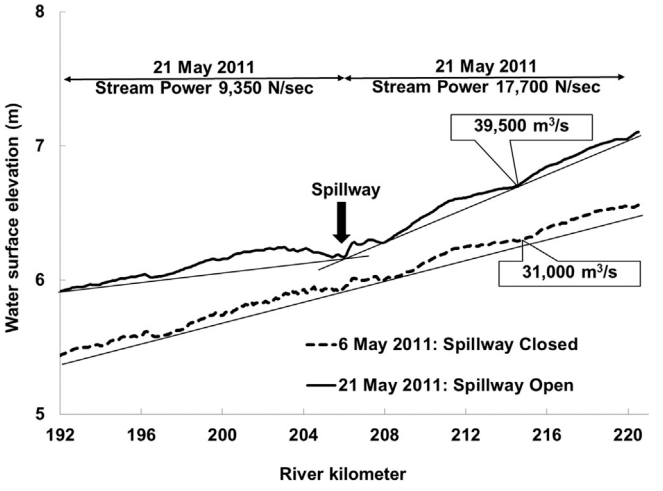

Fig. 10. Model - simulated longitudinal water surface profile on 6 May and 21 May 2011.

5.2. Model calibration and validation

The model was calibrated during the period of 15 March to 15 June 2013 against boat-based field measurements. The field campaign in the ETB site was done as part of the Louisiana Coastal Area (LCA) Mississippi River Hydrodynamic and Delta Management Study and led by the USACE-Engineer Research and Development Center (http://www.lca.gov/Projects/22/). The field observations include multibeam swath bathymetry, ADCP measurements, and sediment concentration at transects between RK 133 and RK 124. Additionally, the stage data at USGS station at Belle Chasse (USGS station ID: 07374525- RK 122) and the USACE station at Algiers Lock (USACE station ID: 01380- RK 142) were used to calibrate the model. Model calibration was accomplished using the data set at the USGS station at Bell Chasse, which includes boat-based field measurements of water discharges and suspended sediment fluxes 12–15 times per year.

The model was validated during the period of 2008 to 2010. The water level data were available at Algiers lock (RK 142) for the entire three years from year 2008 to 2010. However, at Belle Chasse, the stage data were not available from January to October 2008. Hence, the model results were compared with stage data at Belle Chasse from November 2008 to December 2010. For the validation period, only the boat-based suspended sediment load (sand and fine sediment) measurements were available at USGS station at Belle Chasse (a total of 33 measurements) and were thereby used for the model sediment transport validation.

Transverse and vertical velocity profiles calculated by the ETB model are shown in Fig. 11. The model results compared well with field observations. The results showed that the model reproduced the skewedness in the velocity distribution at the outside of the bend near English Turn (RK 126; Fig. 11). The boat collecting ADCP measurements was held stationary at a few locations for ~15–20 min each. The model was able to predict the velocity verticals within the variation observed. This was done to explore the fluctuation of the field velocities. Vertical sediment concentration profiles were collected at these same locations. The model results were compared to the vertical profiles of velocity and sand concentration (Figs. 11B and C).

For the validation effort, the calculated water levels from the year 2008 to 2010 showed reasonable agreement with the field observations. The model was also capable of capturing the order of magnitude and the temporal pattern of fluctuations of the suspended sediment transport (Figs. 12 and 13). Further, the bottom panel (scattered plot) of Fig. 13 shows a direct comparison between the model prediction and measurements. An envelope reflecting a ratio of 0.5 to 2 between predicted and measured loads were drawn around the perfect agreement line. Fig. 13 shows that the model compares well against the measurements for fine material and tends to underpredict the sand load for the smaller loads and agrees better for high sand loads. The statistical analysis conducted to evaluate the model performance is shown in Table 3.

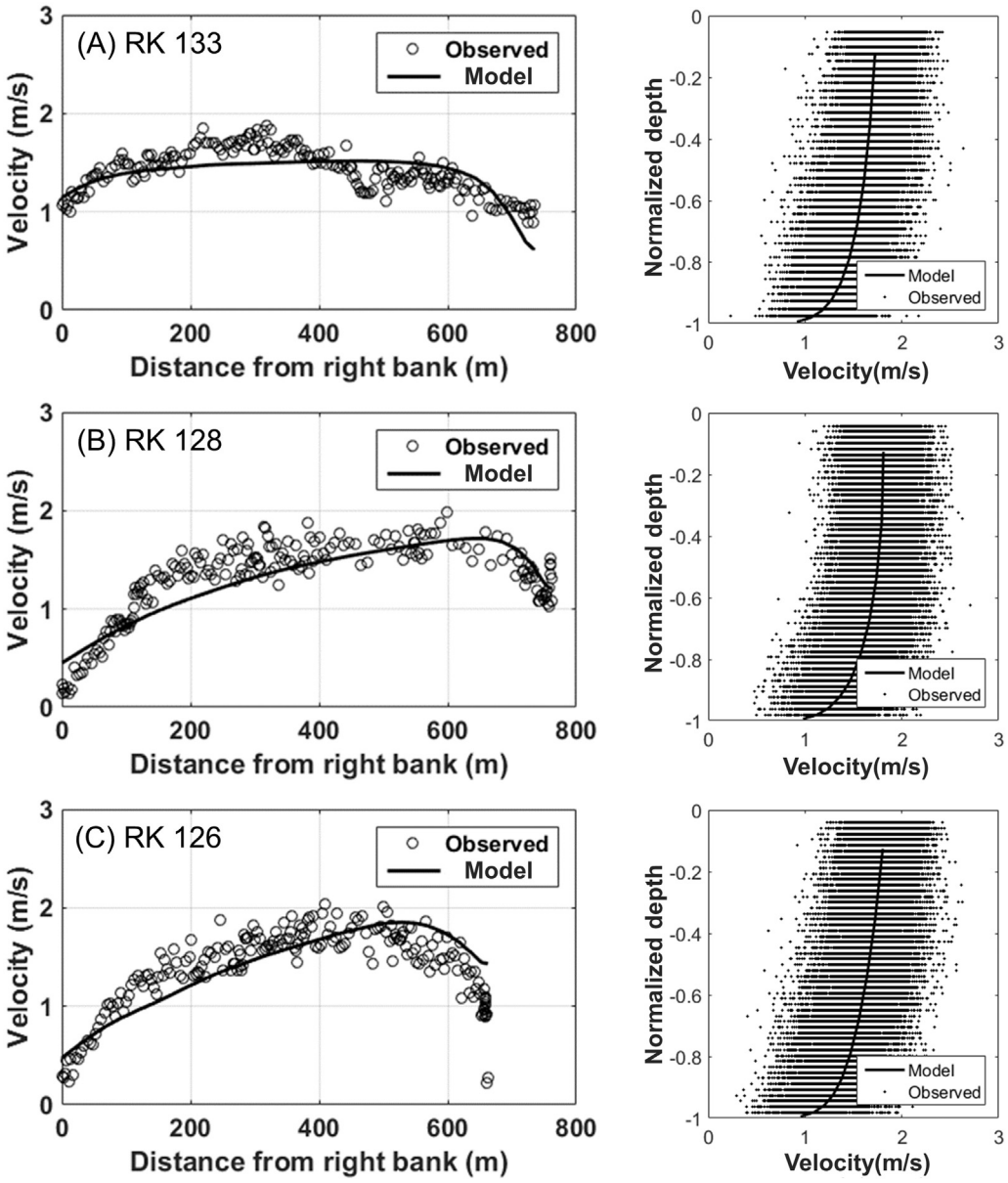

Fig. 11. Comparison between model results and the field observation at RK 126: (A) depth average velocity, (B) vertical velocity profile, and (C) sand concentration profile at RK 126.

5.3. Model applications and analysis

The ETB model was used to perform a 3-year simulation, from the year 2008 to 2010, to examine the performance of a proposed sediment diversion at RK 124 for three different design capacities, namely 7080, 3540, and 2124 m^3/s. The erosion and deposition volumes and sediment budgets were also calculated for each of these experiments and are shown in Figs. 14 and 15. The river channel of the ETB model was divided into nine segments to quantify the volume of the deposition and erosion (river segments are shown in Fig. 1). Fig. 14 shows the deposition in the channel bed, adjacent to, and downstream of the intake in response to the diversion from 2008 to 2010. However, little to no morphologic changes upstream of the diversion intake were observed during this 3-year period. The sediment budget during the years 2008 to 2010 indicated that the diversion size impacts the deposited volume of sand and fine materials on the riverbed (Table 4; Figs. 14 and 15). The amount of material (mostly sand) deposited on the channel bed is proportional to the diversion capacity. The largest capacity examined here is comparable to the analogue. Over the span of three years and multiple flood events, the largest capacity of the proposed diversion deposited approximately the same amount of material on the riverbed as the analogue deposited in a single flood event. Designing the proposed diversion to efficiently capture sand reduced the amount of material deposited on the riverbed downstream of the intake but did not entirely eliminate it. Reduction of the stream power explains the sustained deposition downstream of diversions. Further discussions on the sediment budget and the erosion and deposition patterns for the proposed diversion are provided in the next section.

5.4. Discussions

The SWR was calculated from the model predictions and was limited to flood events with discharge > 17,000 m^3/s (600,000 cfs). This threshold has been determined based on numerous field observations identifying this discharge as the impetus for entraining sand into suspension (Meselhe et al., 2012; Allison et al., 2013). The SWR of fine sediment was ~1.0 during the modeled period confirming the notion that fine material is distributed fairly uniformly within a channel cross section.

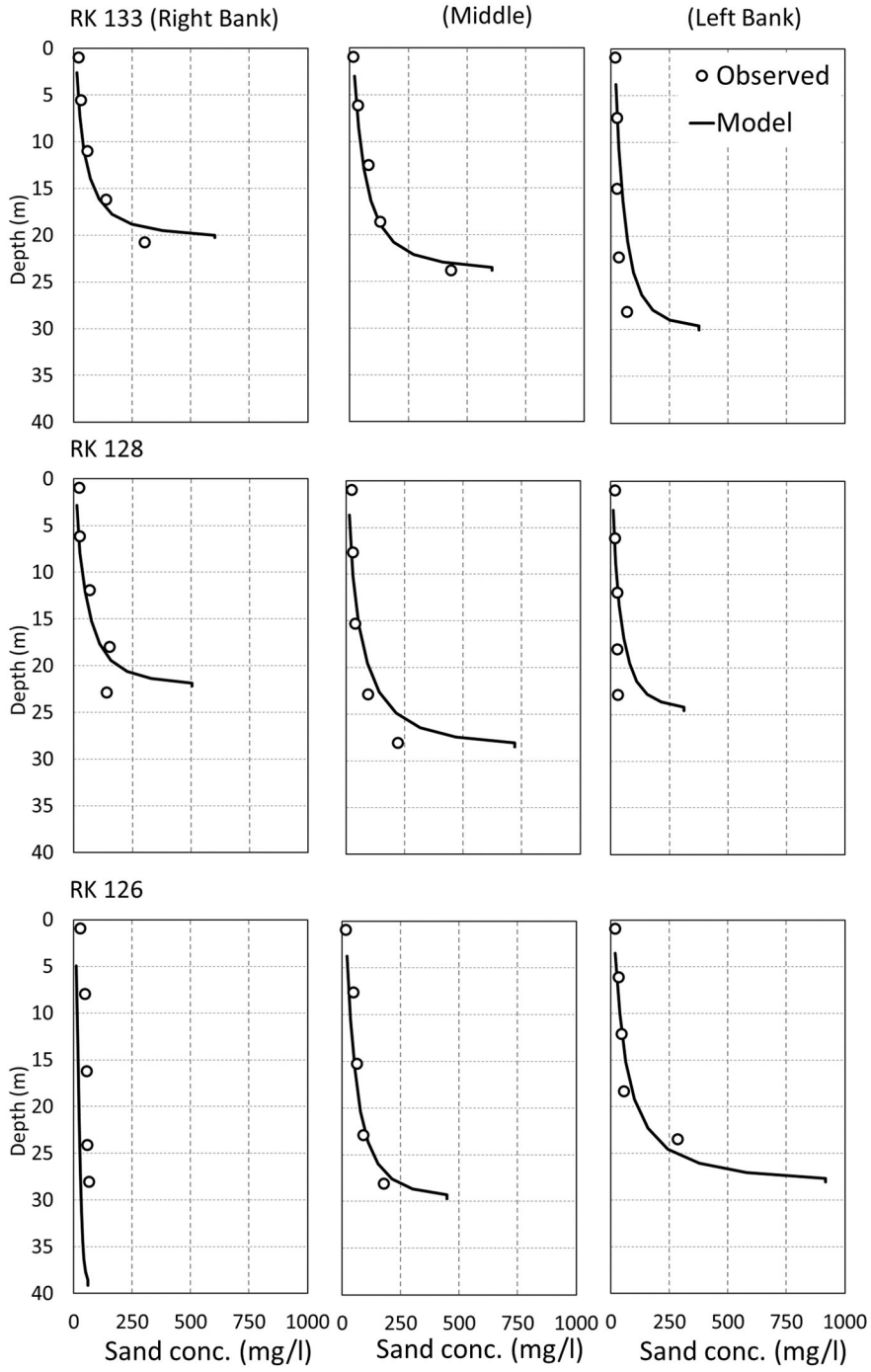

Fig. 12. Comparison between model results and measurements of vertical sand profiles.

The sand SWR was consistently over 2.0 for the three different design capacities at RK 124 and was maximum ~3.0 for the design capacity 3540 m^3/s (Fig. 16). In general, the diversion at all three capacities was efficient in capturing sand from the river. The adequately deep invert elevation, the location of the diversion on top of a sand bar, and the secondary motion generated within the bend at RK 124 helped in capturing large amounts of coarse material from the river channel and augmented the sand SWR for the diversion.

In general, little to no changes upstream of the diversion were observed. This suggests that the diversion does not alter the morphology of the river reach upstream of the diversion intake, at least not during the short-term (i.e., three years) analysis provided by this modeling effort. Similar to the impact of the BC spillway (analogue), the designed diversion also caused deposition adjacent to and downstream of the diversion intake. The sediment budget analysis (Table 4) also shows that the accretion in the river channel is mostly caused by sand. The deposition of sand on the riverbed decreases with the decrease in diversion size. The sediment budget for the 7080 m^3/s (~20–25% of the peak water discharge of 28,320–35,400 m^3/s) diversion shows that 22 million tonnes of sand deposited on the riverbed (45% of the incoming sand load) and 23 million tonnes exited the outfall channel out of 48 million tonnes of sand entering the system. When the diversion size was reduced to 3540 m^3/s (12.5% of the peak water discharge of 28,320 m^3/s), the amount of sand deposited downstream of the diversion was reduced to 21% of the incoming sand load. Further, a reduction in diversion size to 2124 m^3/s (7.5% of the peak water discharge of

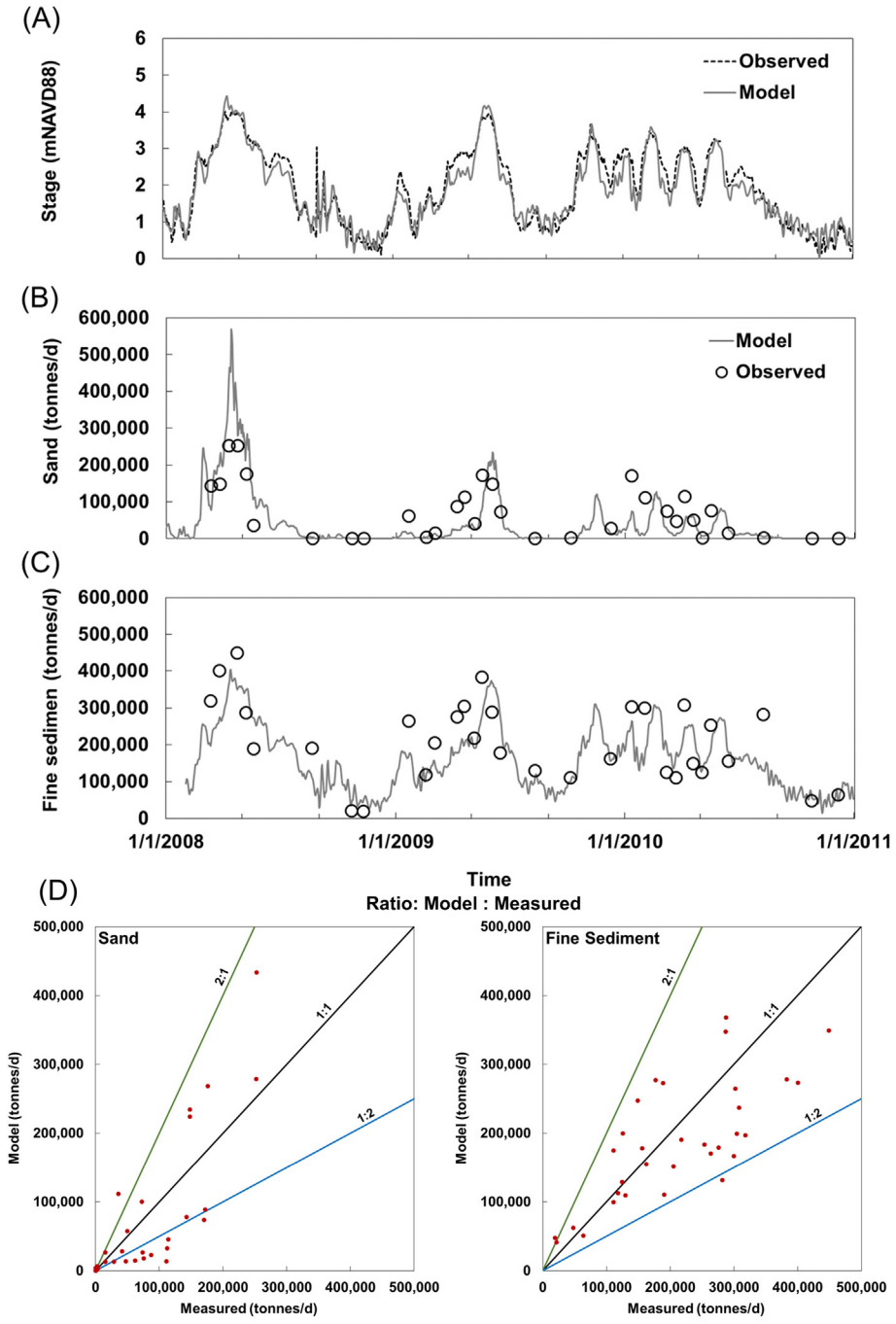

Fig. 13. The ETB model results from 1 Jan 2008 to 1 Jan 2011: (A) Stage at Algiers lock (RK 142); (B) sand load at Belle Chasse (RK 122); and (C) fine sediment load at Belle Chasse (RK 122); bottom panel: scattered plot of measured and predicted sand and fine load at Belle Chasse.

Table 3
Model performance statistics for the ETB model.

Simulation period	Model output	Bias %	RMSE%	Correlation coefficient
March–June 2013	Velocity (transverse profile)	3.2%	24.0%	0.8
	Velocity (vertical profile)	9.1%	61.0%	0.9
	Water level	−0.4%	2.6%	1.0
	Sand load	3.0%	N/A[a]	N/A
	Fine load	−2.0%	N/A	N/A
January 2008–December 2011	Water level	−2.0%	21.0%	1.0
	Sand load	−7.0%	81.0%	0.8
	Fine load	−16.0%	46.0%	0.7

[a] Inadequate sample to calculate statistics.

28,320 m^3/s) caused sand deposition on the riverbed downstream of the diversion in the amount of 13% of the incoming sand load. Hence, the size of the diversion also affects the magnitude of the deposition in the river downstream of the intake because of the change in stream power loss for the diversion. These results indicate that the improvement in the sand capture efficiency may reduce the deposition downstream of diversion intakes, but it would not eliminate it except in extreme cases. The reduction in the stream power will almost always trigger deposition downstream of diversion intakes.

To investigate the importance of placing a diversion on top of a sand bar, the diversion was moved to RK 131 at the outside of a meander bend, right across a point bar. The test was done with a diversion discharge capacity of 7080 m^3/s and the invert elevation at −12.91 m NAVD88. Placement of the diversion at RK 131 reduced the sand SWR

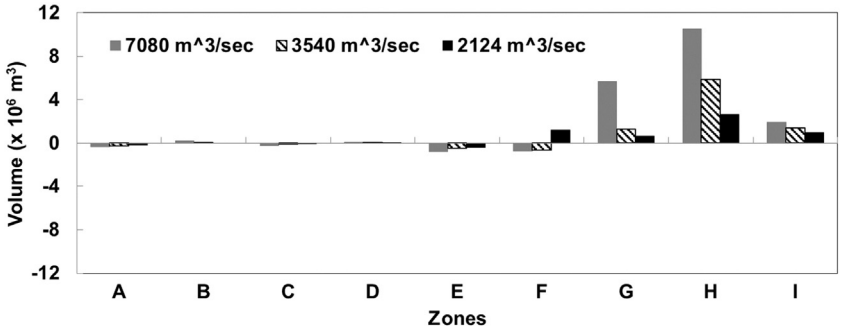

Fig. 14. River segments considered to quantify morphologic changes for the ETB model.

to 0.5 and evidently supported the importance of placing diversions on top of a sand bar at RK 124 to enhance the sand capture efficiency (Fig. 17). The sediment budget for this test indicates that ~152 million tonnes of sediment was deposited on the riverbed for the diversion, which was significantly more than the deposition quantity when the diversion was placed on top of a sand bar at RK 124. Clearly the low sand capture efficiency increased the deposition amount on the riverbed downstream of the diversion intake.

Another test was performed with the same diversion capacity and intake invert elevation by retaining the original location of the diversion at RK 124 while artificially straightening the channel to examine the effect of the secondary motion strength on the sand capture efficiency

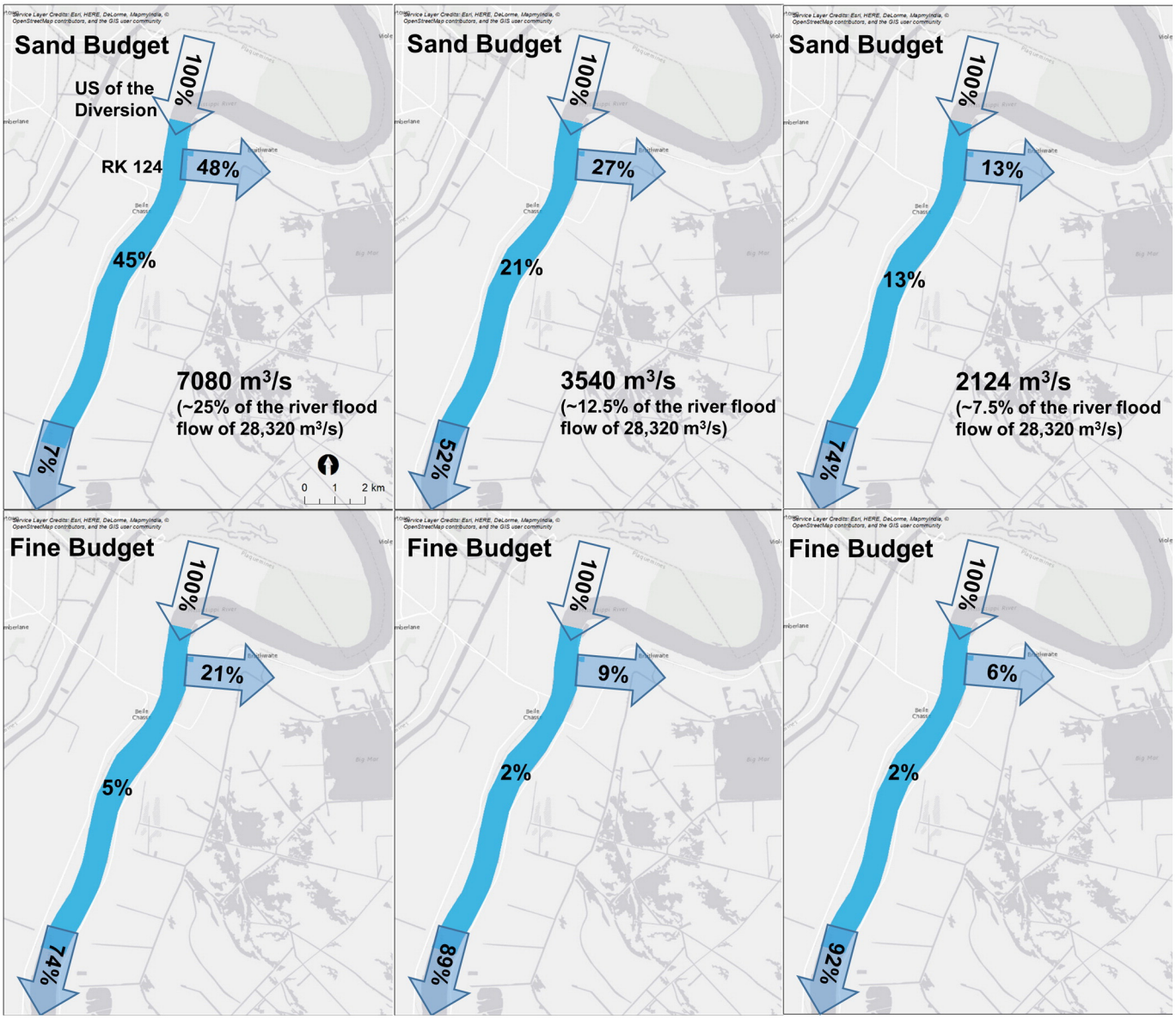

Fig. 15. Sand and fine material budget for the proposed diversion (at ETB) for three design capacities.

Table 4
Sediment budget over a 3-year period (2008 through 2010) for the ETB model.

Sediment type	Sediment	Inflow US of the diversion	Outflow DS of the diversion	Deposited on the riverbed	Diverted
Diversion size: 7080 m^3/s					
Sand	Mass (10^6 tonnes)	48	3	22	23
	% of U/S	100%	7%	45%	48%
Fine Sediment	Mass (10^6 tonnes)	179	133	9	37
	% of U/S	100%	74%	5%	21%
Total	Mass (10^6 tonnes)	227	136	31	60
	% of U/S	100%	60%	14%	26%
Diversion size: 3540 m^3/s					
Sand	Mass (10^6 tonnes)	48	25	10	13
	% of U/S	100%	52%	21%	27%
Fine Sediment	Mass (10^6 tonnes)	179	158	4	17
	% of U/S	100%	89%	2%	9%
Total	Mass (10^6 tonnes)	227	183	14	30
	% of U/S	100%	81%	6%	13%
Diversion size: 2124 m^3/s					
Sand	Mass (10^6 tonnes)	48	36	6	6
	% of U/S	100%	74%	13%	13%
Fine Sediment	Mass (10^6 tonnes)	179	164	4	11
	% of U/S	100%	92%	2%	6%
Total	Mass (10^6 tonnes)	227	200	10	17
	% of U/S	100%	88%	4%	8%

(Fig. 18). Straightening the channel does not eliminate the presence of the secondary motion, however, it should significantly weaken it. The purpose of this test is to investigate the impact of the secondary motion on the flow pattern near the diversion intake, the bed shear stress spatial distribution and ultimately on the sand capture efficiency. The SWR for the original (curved) river and for the straightened channel are shown in Fig. 18. The comparison between sediment budgets also shows that the original diversion diverts 14% of the U.S. sand loads more than the artificially straightened channel.

Typically in sharply curved bends, the locus of high streamwise velocities shifts outward, and the retarded fluid moves close to the inner bank, resulting in strong transverse velocity and high bed shear stress (Koken et al., 2013). Further, high curvature bends, namely with $R/B < 3$ (R = radius of the curve, and B = width of the channel) exhibit strong secondary motion and high bed shear stress leading to more bed erosion than the milder bends (Kashyap et al., 2012). The model results displays these patterns (Figs. 19, 20). The curved channel considered for this numerical experiment is considered to have high curvature ($R/B \sim 1.7$). In Fig. 19, the curved channel shows higher bed shear stress leading to more entrainment of sand into suspension and potentially available for capture by the diversion. Fig. 20 shows contour maps of the velocity components, the turbulence energy and the sand concentration at XS-1 immediately upstream of the diversion intake (location of XS-1 is shown in Fig. 19). The invert of the diversion intake is shown on the cross sections. The transverse and vertical velocities in the curved channel are stronger than in the straightened channel illustrating the strength of the secondary motion. Fig. 20D shows higher turbulence energy reaching the upper layers of the water column in the curved channel. The secondary motion along with the turbulence energy resulted in higher sand concentrations in the upper layers of the water column adjacent to the diversion intake. These will likely lead to the capture of higher sand amounts into the diversion in the curved channel case than the straightened channel. This test illustrates that it would be beneficial, whenever possible, to locate sediment diversions, not only on a sand bar, but also on the inside of a meander. Such location maximizes the capture efficiency of sand.

6. Conclusions

The analyses in this paper provide insights toward understanding the riverside hydrodynamics and morphodynamics in the vicinity of large diversions. It also identifies key parameters that influence the river response to large water and sediment pulses and impact the sand capture efficiency. The analysis includes the setup, calibration, validation, and application of three-dimensional morphodynamic models to an existing large, diversion (used here as an analogue) on the lower Mississippi River and to proposed/hypothetical sediment diversions. The morphodynamic models, supported by detailed field observations, were used to provide insights into the potential morphologic response of rivers to large, pulsed diversions. The analyses presented here shows that sand capture efficiency and stream power loss calculations are good indicators for the riverside morphologic response to pulsed sediment diversions. A capture efficiency of unity or higher would mean that the sand concentration in the diverted water is similar to or higher than the average sand concentration in the main river. To minimize riverine deposition, an SWR higher than unity is desired. However, high SWR does not eliminate deposition downstream of diversions, as loss of stream power would likely induce aggradation on the riverbed.

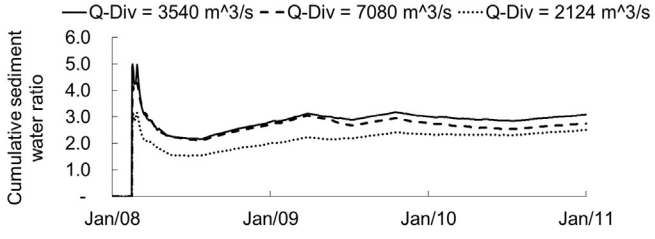

Fig. 16. Sand SWR comparison at three different capacities at RK 124 from the year 2008 to 2010 for the ETB model.

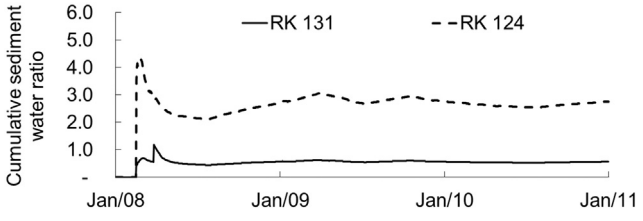

Fig. 17. Sand SWR comparison for different locations at capacity 7080 m^3/s from the year 2008 to 2010.

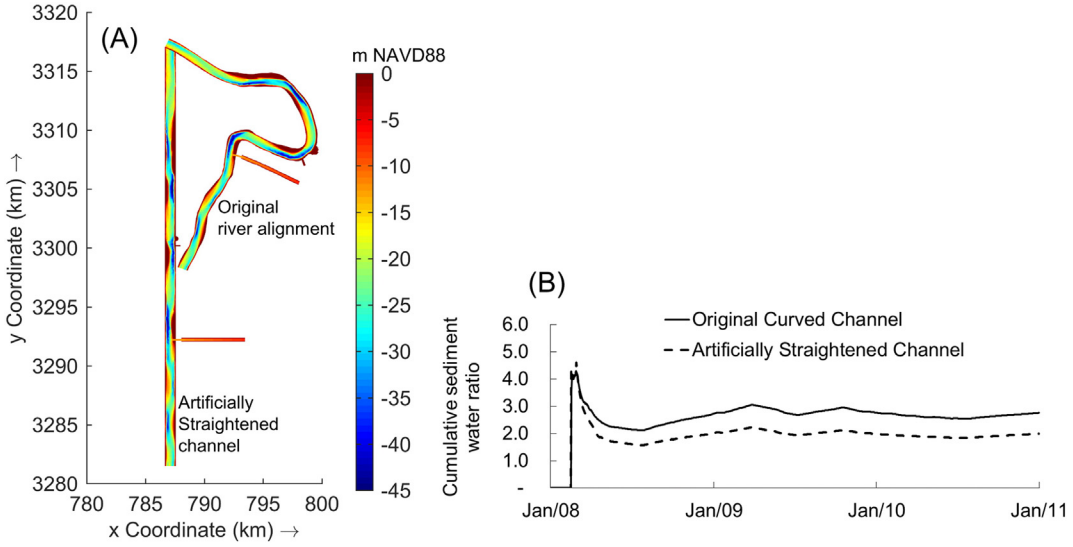

Fig. 18. Comparison of sediment water ratio between the original curved channel and the artificially straightened channel.

The validated model reasonably captured the local sediment dynamics adjacent to and downstream of the diversion analogue (Bonnet Carré spillway). The model supported by field measurements showed that the disproportionate extraction of water and sand contributed to the deposition within the river channel immediately downstream of the diversion intake. For the diversion analogue, the sand capture efficiency was ~0.5, and the stream power reduction was also significant. These factors to a large degree explain the aggradation behavior immediately downstream of the BC spillway intake.

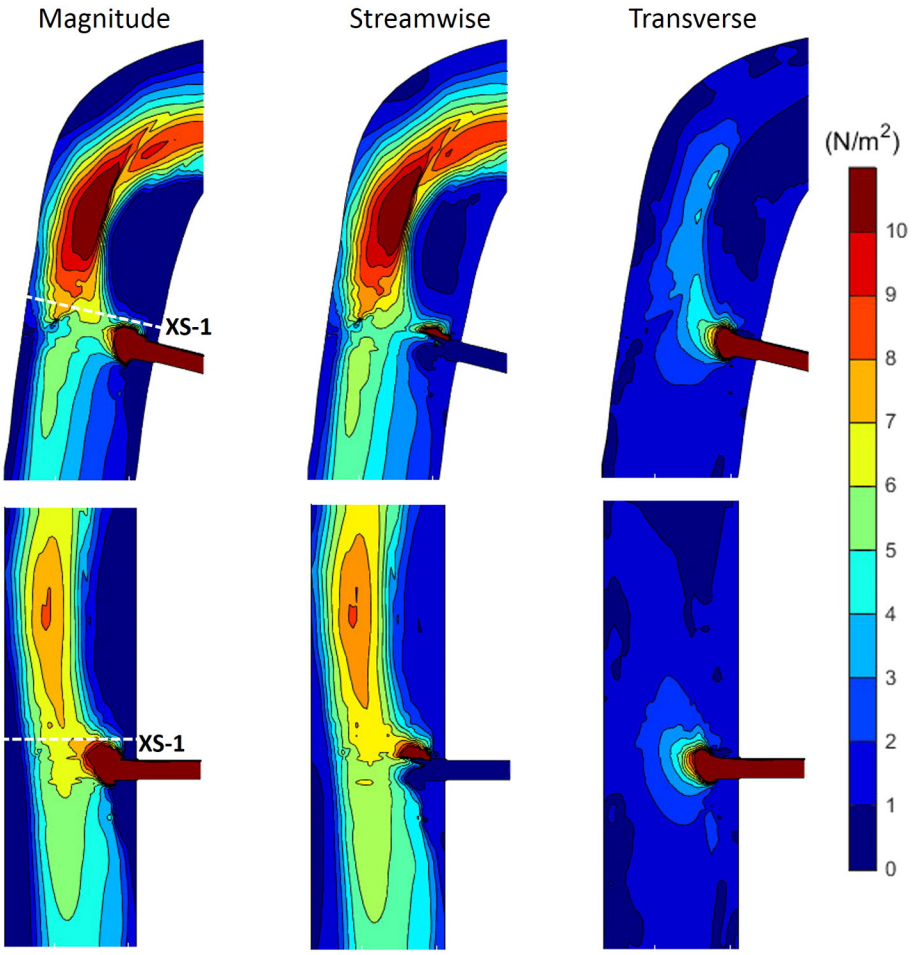

Fig. 19. Bed shear stress, total magnitude (left), and the components: streamwise (center) and transverse (right) near the intake of the diversion for the original curved channel (top) and the artificially straight channel (bottom).

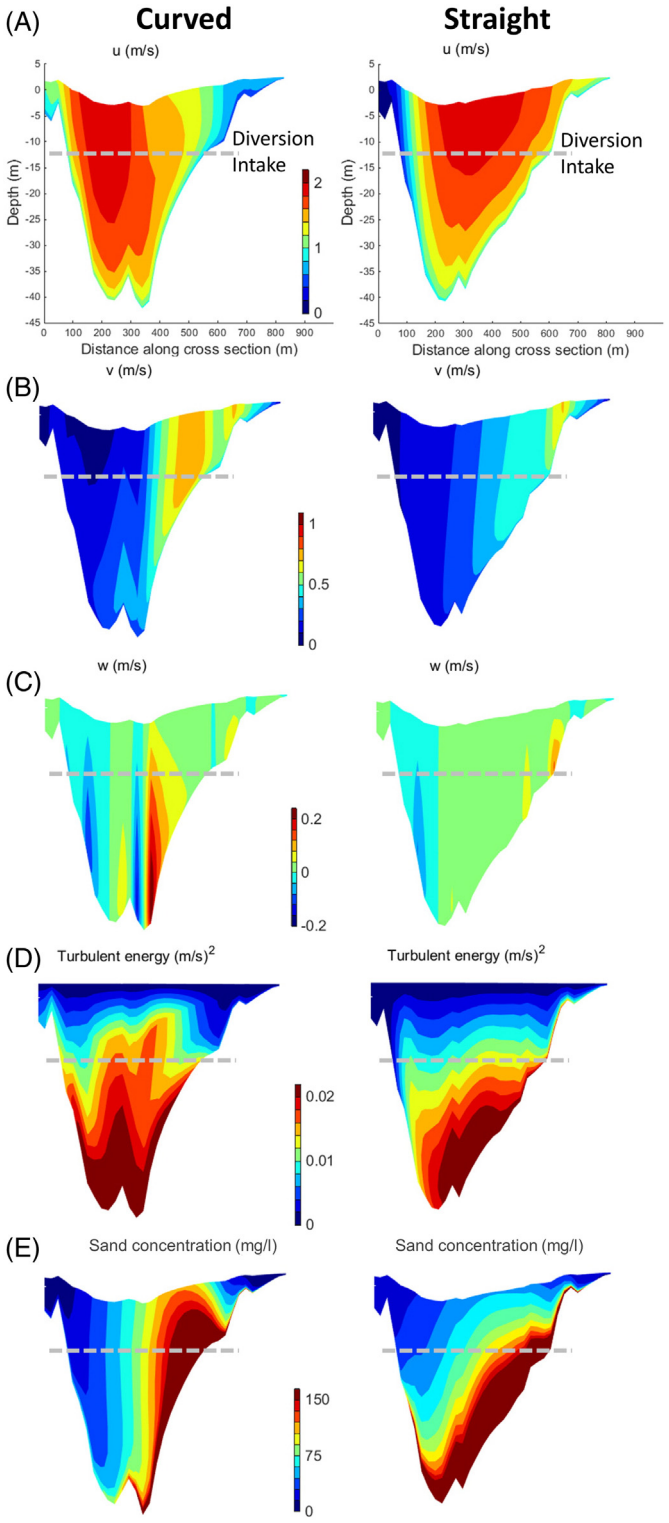

Fig. 20. Velocity, turbulent energy and sand concentration contour at XS-1: (A) streamwise velocity, (B) transverse velocity, (C) vertical velocity, (D) turbulent energy, and (E) suspended sand concentration.

Further analysis showed that sand capture efficiency of diversions increases when the diversion intake is sufficiently deep. That was evident when the intake of the proposed diversion was set at an elevation of −12.91 m NAVD88, compared to the diversion analogue invert elevation of ~0.0 m NAVD88.

The numerical experiments performed as part of this study showed little to no changes upstream of the diversion intake. This suggests that the diversion does not alter the morphology of the upstream river reach, at least during the short-term (three years) analysis. However, accretion occurred adjacent to and downstream of the intake in the river because of the stream power loss for large-scale diversions, regardless of the sand capture efficiency. High sand capture efficiency, indeed, lowers the magnitude of the downstream deposition, but it does not eliminate it.

The analysis performed here also showed that the intake placement on top of a sand bar significantly (and favorably) impacts the sand capture efficiency. Additionally, it is beneficial to locate sediment diversions on the inside of a meander to take advantage of the secondary motion and increased bed shear stress leading to significant increase in entrainment of sand into suspension and getting captured by the diversion.

The analysis also showed that the fine sediment capture efficiency was 1.0 in all the locations studied here. This confirms the notion that timing, and not location, is the key parameter to increase the amount of fine material to be diverted from a channel to the adjacent basins. Specifically, coordinating the timing of operating sediment diversions relative to the incoming fine material hydrograph is important.

Acknowledgements

This research was funded in part through an NSF EPSCOR Grant # EPS-1010640 and the Louisiana Board of Regents, and also in part through the Louisiana Coastal Protection and Restoration Authority (CPRA) (MR-0016). The latter phase of the modeling and field observations were funded through the Mississippi River Hydrodynamics and Delta Management Study, jointly funded by the U.S. Army Corps of Engineers and CPRA and through the Science and Engineering Plan (SEP), funded by the Baton Rouge Area Foundation (BRAF) and CPRA. The authors would like to thank the Engineer Research and Development Center (ERDC), especially Mr. Thad Pratt for providing data to validate the numerical models, and to Deltares for technical discussions, especially related to the morphological module of Delft3D. The authors also like to sincerely thank the reviewers and the editor of the journal for their helpful comments and suggestions that resulted in significant improvements to this manuscript.

References

Allison, M.A., Meselhe, E.A., 2010. The use of large water and sediment diversions in the lower Mississippi River (Louisiana) for coastal restoration. J. Hydrol. 387 (3), 346–360.

Allison, M.A., Demas, C.R., Ebersole, B.A., Kleiss, B.A., Little, C.D., Meselhe, E.A., Powell, N.J., Pratt, T.C., Vosburg, B.A., 2012. A water and sediment budget for the lower Mississippi–Atchafalaya River in flood years 2008–2010: implications for sediment discharge to the oceans and coastal restoration in Louisiana. J. Hydrol. 432, 84–97.

Allison, M.A., Vosburg, B.M., Ramirez, M.T., Meselhe, E.A., 2013. Mississippi River channel response to the Bonnet Carré Spillway opening in the 2011 flood and its implications for the design and operation of river diversions. J. Hydrol. 477, 104–118.

Allison, M.A., Ramirez, M.T., Meselhe, E.A., 2014. Diversion of Mississippi River water downstream of New Orleans, Louisiana, USA to maximize sediment capture and ameliorate coastal land loss. Water Resour. Manag. 28 (12), 4113–4126.

Bagnold, R.A., 1966. An Approach to the Sediment Transport Problem from General Physics (Geological Survey Professional Paper). U.S. Geological Survey, U. S. Govt. Print. Off.

Barras, J.A., 2006. Land area change in coastal Louisiana after the 2005 hurricanes: a series of three maps. US Geological Survey Open File Report 06-1274.

Barras, J.A., 2009. Land Area Change and Overview of Major Hurricane Impacts in Coastal Louisiana, 2004–08: U.S. Geological Survey Scientific Investigations Map 3080, scale 1:250,000, 6 p. pamphlet.

Barras, J.A., Beville, S., Britsch, D., Hartley, S., Hawes, S., Johnston, J., Kemp, P., Kinler, Q., Martucci, A., Porthouse, J., Reed, D., Roy, K., Sapkota, S., Suhayda, J., 2003. Historical and projected coastal Louisiana land changes: 1978–2050. U.S. Geological Survey Open File Report 03–334 (39 pp.).

Bos, M.F.M., 2011. The Morphological Effects of Sediment Diversions on the Lower Mississippi River (MSc Thesis) Delft University of Technology, the Netherlands.

Britsch, L.D., Kemp, E.B., 1990. Land loss rates: mississippi river deltaic plain. Technical Report GL-90-2. US. Army Engineer Waterways Experiment Station, Vicksburg, MS (25 pp.).

Caldwell, R.L., Edmonds, D.A., 2014. A numerical modeling study of the effects of sediment properties on deltaic processes and morphology. J. Geophys. Res. Earth Surf. 119. http://dx.doi.org/10.1002/2013JF002965.
Coleman, J.M., Roberts, H.R., Stone, G.W., 1998. The Mississippi River delta; an overview. J. Coast. Res. 14 (3), 698–716.
Couvillion, B.R., Beck, H., 2013. Marsh collapse thresholds for coastal Louisiana estimated using topography and vegetation index data. J. Coast. Res. 63 (sp1), 58–67.
CPRA (Coastal Protection and Restoration Authority), 2012. Louisiana's Comprehensive Master Plan for a Sustainable Coast (Baton Rouge, State of Louisiana 190 pp.).
Day, J.W., Shaffer, G.P., Britsch, L.D., Reed, D.J., Hawes, S.R., Cahoon, D., 2000. Pattern and process of land loss in the Mississippi Delta: a spatial and temporal analysis of wetland habitat change. Estuaries 23 (4), 425–438.
Day, J.W., Boesch, D.F., Clairain, E.J., Mitsch, W.J., Orth, K., Mashriqui, H., Reed, D.J., Shabman, L., Simenstad, C.A., Streever, B.J., Twilley, R.R., Watson, C.C., Wells, J.T., Whigham, D.F., 2007. Restoration of the Mississippi Delta: lessons from Hurricanes Katrina and Rita. Science 315 (5819), 1679–1684.
Deltares, 2011. Simulation of multi-dimensional hydrodynamic flows and transport phenomena, including sediments. User Manual Delft-3D Flow.
Edmonds, D.A., Slingerland, R.L., 2007. Mechanics of river mouth bar formation: implications for the morphodynamics of delta distributary networks. J. Geophys. Res. Earth Surf. 112. http://dx.doi.org/10.1029/2006JF000574.
Edmonds, D.A., Slingerland, R.L., 2010. Significant effect of sediment cohesion on delta morphology. Nat. Geosci. 3 (2), 105–109. http://dx.doi.org/10.1038/NGE0730.
Fabre, J.B., 2012. Sediment Flux & Fate for a Large-Scale Diversion: the 2011 Mississippi River Flood, the Bonnet Carré Spillway, and the Implications for Coastal Restoration in South Louisiana (MSc. Thesis) Louisiana State University, USA.
Fan, H., Huang, H., Zeng, T., 2006. Impacts of anthropogenic activity on the recent evolution of the Huanghe (yellow) river delta. J. Coast. Res. 224, 919–929.
Gagliano, S., Meyer-Arendt, K., Wicker, K., 1981. Land loss in the Mississippi River delta plain. Trans.-Gulf Coast Assoc. Geol. Sci. 31, 295–300.
Garcia, M.H., 2008. Sedimentation engineering processes, measurements, modeling, and practice. ASCE Manuals and Reports on Engineering Practice No. 110. American Society of Civil Engineers (ISBN: 978–0–7844-0814-8).
Gaweesh, A.M., Meselhe, E.A., 2016. Evaluation of sediment diversion design attributes and their impact on the capture efficiency. J. Hydraul. Eng. 04016002 http://dx.doi.org/10.1061/(ASCE)HY.1943–7900.0001114.
Kamruzzaman, M., Beecham, S., Zuppi, G.M., 2012. A model for water sharing in the Ganges river basin. Water Environ. J. 26, 308–318.
Kashyap, S., Constantinescu, G., Rennie, C.D., Post, G., Townsend, R., 2012. Influence of channel aspect ratio and curvature on flow, secondary circulation and bed shear stress in a rectangular channel bend. J. Hydraul. Eng. 138 (12), 1045–1059. http://dx.doi.org/10.1061/ (ASCE) HY.1943-7900.0000643.
Khaiashy, K.E., McCorquodale, J.A., Georgiou, I., Meselhe, E.A., 2010. Three dimensional hydrodynamic modeling over bed forms in open channels. Int. J. Sediment Res. 25 (4), 431–440. http://dx.doi.org/10.1016/S1001-6279(11)60010-3.
Koken, M., Constantinescu, G., Blanckaert, K., 2013. Hydrodynamic processes, sediment erosion mechanisms, and Reynolds-number-induced scale effects in an open channel bend of strong curvature with flat bathymetry. J. Geophys. Res. Earth Surf. 118, 2308–2324. http://dx.doi.org/10.1002/2013JF002760.
Kolker, A.S., Cable, J.E., Johannesson, K.H., Allison, M.A., 2013. Pathways and processes associated with the transport of groundwater in deltaic systems. J. Hydrol. 498 (2013), 319–334.
Lesser, G.R., Roelvink, J.A., Van Kester, J.A.T.M., Stelling, G.S., 2004. Development and validation of a three-dimensional morphological model. Coast. Eng. 51 (8), 883–915.
Meselhe, E.A., Rodrigue, M.D., 2013. Models Performance Assessment Metrics and Uncertainty Analysis. Louisiana Coastal Area Program Mississippi River Hydrodynamics and Delta Management Study (http://www.lca.gov/Projects/22/Default.aspx).
Meselhe, E.A., Georgiou, I., Allison, M.A., McCorquodale, J.A., 2012. Numerical modeling of hydrodynamics and sediment transport in lower Mississippi at a proposed delta building diversion. J. Hydrol. 472–473, 340–354.
Meselhe, E.A., McCorquodale, J.A., Shelden, J., Dortch, M., Brown, T.S., Elkan, P., Rodrigue, M.D., Schindler, J.K., Wang, Z., 2013. Eco-hydrology component of Louisiana's 2012 coastal master plan: mass-balance compartment model. J. Coast. Res. 67 (sp), 16–28.
Mirza, M.M.Q., 1998. Diversion of the Ganges water at Farakka and its effects on salinity in Bangladesh. Environ. Manag. 22, 711–722.
Morton, R., Tiling, G., Ferina, N., 2003. Causes of hotspot wetland loss in the Mississippi delta plain. Environ. Geosci. 10, 71–80.
Morton, R., Bernier, J., Barras, J.A., 2006. Evidence of regional subsidence and associated interior wetland loss induced by hydrocarbon production, Gulf coast region, USA. Environ. Geol. 50, 261–274.
Mossa, J., 1989. Hysteresis and nonlinearity of discharge–sediment relationships in the Atchafalaya and lower Mississippi Rivers. Sediment and the Environment. Proceedings of the Baltimore Symposium, IAHS Publ. no. 184.
Partheniades, E., 1965. Erosion and deposition of cohesive soils. J. Hydraul. Div. ASCE 91 (HY 1), 105–139 (79, 329, 569).
Penland, S., Williams, S.J., Davis, D.W., Sallenger Jr., A.H., Groat, C.G., 1992. Barrier island erosion and wetland loss in Louisiana. Atlas of shoreline changes in Louisiana from 1985 to 1989. US Geological Survey, Miscellaneous Investigations Series I-1250A, pp. 2–7.
Rahman, M.M., Varis, O., 2009. Integrated water management of the Brahmaputra basin: perspectives and hope for regional development. Nat. Res. Forum 33, 60–75.
Ramirez, M.T., Allison, M.A., 2013. Suspension of bed material over sand bars in the lower Mississippi River and its implications for Mississippi Delta environmental restoration. J. Geophys. Res. Earth Surf. 118, 1–20. http://dx.doi.org/10.1002/jgrf.20075.
Reed, D.J., 2002. Sea-level rise and coastal marsh sustainability: geological and ecological factors in the Mississippi Delta plain. Geomorphology 48, 233–243.
Rivera-Monroy, V.H., Branoff, B., Meselhe, E.A., McCorquodale, A., Dortch, M., Steyer, G.D., Visser, J., Wang, H., 2013. Landscape-level estimation of nitrogen loss in coastal Louisiana wetlands: potential sinks under different restoration scenarios. J. Coast. Res. 67 (sp), 75–87.
Steyer, G.D., Sasser, C.E., Visser, J.M., Swensen, E.M., Nyman, J.A., Raynie, R.C., 2003. A proposed coast-wide reference monitoring system for evaluating wetland restoration trajectories in Louisiana. Environ. Monit. Assess. 81, 107–117.
Steyer, G.D., Couvillion, B., Wang, H., Sleavin, W., Rybczyk, J., Trahan, N., Beck, H., Fischenich, C., Boustany, R., Allen, Y., 2012. Louisiana's 2012 Coastal Master Plan: Wetland Morphology Model Technical Report. Louisiana Coastal Protection and Restoration Authority (CPRA), Baton Rouge, Louisiana (http://www.coastalmasterplan.louisiana.gov/).
Sutherland, J., Walstra, D.J.R., Chesher, T.J., Van Rijn, L.C., Southgate, H.N., 2003. Evaluation of coastal area modelling systems at an estuary mouth. Coast. Eng. 119–142 (doi: 51 (2004)).
Syvitski, J.P.M., Kettner, A.J., Overeem, I., Hutton, E.W.H., Hannon, M.T., Brakenridge, G.R., Day, J., Vorosmarty, C., Saito, Y., Giosan, L., Nicholls, R.J., 2009. Sinking deltas due to human activities. Nat. Geosci. http://dx.doi.org/10.1038/NGE0629.
Turner, R.E., 1997. Wetland loss in the Northern Gulf of Mexico. Estuaries 20 (1), 1–13.
Van Rijn, L.C., 1984a. Sediment transport, part I: bedload transport. J. Hydraul. Eng. 110 (10), 1431–1456.
Van Rijn, L.C., 1984b. Sediment transport, part II: suspended load transport. J. Hydraul. Eng. 110 (11), 1613–1638.
Visser, J.M., Duke-Sylveste, S.M., Carter, J., Broussard III, W.P., 2013. A model to forecast wetland vegetation changes resulting from coastal restoration and protection in coastal Louisiana. J. Coast. Res. 67 (sp), 51–59.